Elektrophysiologische Charakterisierung des isolierten circadianen Schrittmachers der Schabe *Leucophaea maderae*

Electrophysiological characterization of the isolated circadian pacemaker of the cockroach *Leucophaea maderae*

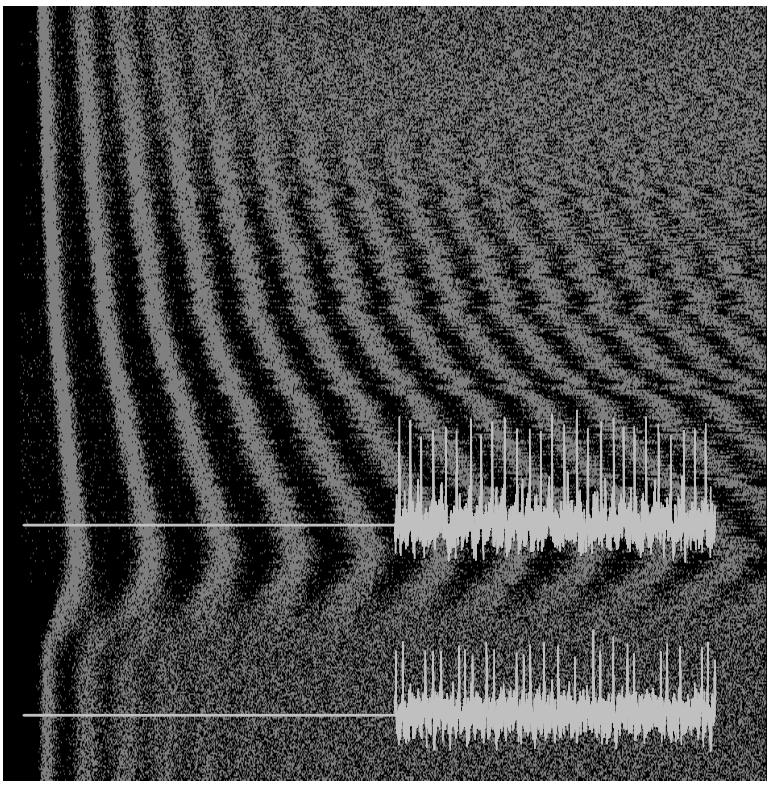

Dissertation zur Erlangung des Doktorgrades der Naturwissenschaften (Dr. rer. nat.)
dem Fachbereich Biologie der Philipps-Universität Marburg vorgelegt von

Nils-Lasse Schneider
aus Freudenberg

Marburg/Lahn
2005

Elektrophysiologische Charakterisierung des isolierten circadianen Schrittmachers der Schabe *Leucophaea maderae*

Electrophysiological characterization of the isolated circadian pacemaker of the cockroach *Leucophaea maderae*

Dissertation
zur
Erlangung des Doktorgrades
der Naturwissenschaften
(Dr. rer. nat.)

dem
Fachbereich Biologie
der Philipps-Universität Marburg
vorgelegt von

Nils-Lasse Schneider
aus Freudenberg

Marburg/Lahn
2005

Vom Fachbereich Biologie der Philipps-Universität Marburg als Dissertation am

12.12.2005 angenommen.

Erstgutachter Apl. Prof. Dr. Monika Stengl
Zweitgutachter Prof. Dr. Uwe Homberg

Tag der mündlichen Prüfung am 26.01.2006.

Solange der Gang des Uhrwerkes nicht ganz aufhört, wird keine Unregelmäßigkeit oder Verzögerung im Gang der Uhr zu fürchten sein; die Uhr wird die Zeit stets messen oder sie wird sie überhaupt nicht messen.

Christiaan Huygens, 1667

Inhaltsverzeichnis

Chapter III 37

Zusammenfassung

Der Sitz des circadianen Schrittmachers, der das Laufverhalten der Schabe *Leucophaea maderae* steuert, wurde durch Läsions- und Transplantationsexperimente in der akzessorischen Medulla (aMe; Plural akzessorische Medullae, aMae) lokalisiert. Die aMe ist ein noduläres Neuropil, welches sich am frontalen, ventromedialen Rand der Medulla in den bilateralen optischen Loben befindet. Immunfärbungen gegen das Octadeca-Peptid *pigment-dispersing hormon* (PDH) aus Crustaceen zeigen eine dichte Innervation von PDH-immunreaktiven (PDH-ir) Zellen in der aMe. Bei *Drosophila melanogaster* und *Leucophaea maderae* exprimiert ein Grossteil der PDH-ir Zellen das Protein *PERIOD*, einen integralen Bestandteil des molekularen circadianen Schrittmachers (*pacemaker*). Darüber hinaus erfüllt die Anatomie der gefundenen PDH-ir Zellen wichtige Kriterien eines circadianen Schrittmachers. So weisen sie Projektionen in der Lamina auf und somit einen möglichen Informationsausgang zu den Komplexaugen, es besteht eine Kopplungsbahn zwischen den bilateralen aMae und es sind Ausgänge in das superiore mediane Protocerebrum vorhanden, welche für die Kontrolle des Verhaltens verantwortlich sein könnten.

Zusätzlich zu den PDH-ir Zellen wird die aMe von einer Vielzahl verschiedener Peptid- und GABA-ir Neurone innerviert. Die Verzweigungen dieser Neurone formen Subkompartimente in der aMe: ein dichtes noduläres Neuropil, dazwischen ein internoduläres Neuropil und eine „Schale“, die das noduläre und internoduläre Neuropil umgibt. Das noduläre Neuropil weist dichte Verzweigungen aus dem GABA-ir distalen Trakt auf, die vermutlich für die Lichtsynchronisation verantwortlich sind. Zusätzliche Verzweigungen von circa 25 GABA-ir Neuronen mit Somata in direkter Nähe zur aMe dienen wahrscheinlich als lokale Interneurone.

In den letzten Jahren wurden große Fortschritte in der Erforschung des molekularen Schrittmachers gemacht, aber nur wenige Informationen zu den physiologischen Eigenschaften der Schrittmacherneurone und deren Verschaltung zu einem neuronalen Netzwerk sind bekannt. In der vorliegenden Dissertation wurde eine Methode entwickelt und etabliert, welche es ermöglicht, über einen Zeitraum von Stunden bis hin zu mehreren Tagen die elektrische Aktivität von isolierten aMae aufzuzeichnen. Mit dieser Methode werden mit einer niederohmigen Saugelektrode Summenpotentiale von mehreren Neuronen simultan extrazellulär abgeleitet (*multi-unit recording*). Dies ermöglicht, die zeitliche Koordination der elektrischen Aktivität von Neuronen in einem Netzwerk zu untersuchen.

Das Ziel der Arbeit war die elektrophysiologische und pharmakologische Charakterisierung der aMe und die Untersuchung, ob das neuronale Netzwerk der isolierten aMe selbstständig einen circadianen Rhythmus generiert.

Die vorliegende Dissertation gliedert sich in drei Kapitel:

Kapitel I: *Pigment-dispersing factor* and GABA synchronisieren Zellen der isolierten circadianen Uhr der Schabe *Leucophaea maderae*

(Pigment-dispersing factor and GABA synchronize cells of the isolated circadian clock of the cockroach *Leucophaea maderae*)

Extrazelluläre Langzeitableitungen von Summenpotentialen von isolierten aMae der Schabe *Leucophaea maderae* zeigten, dass die Mehrzahl der abgeleiteten Neurone spontanaktiv Aktionspotentiale mit sehr regelmäßigen Intervallen im Millisekundenbereich generieren. Diese Regelmäßigkeit wird wahrscheinlich durch Membranpotentialoszillationen mit ultradianen Periodenlängen verursacht. Die meisten Neurone in der aMe sind zu Ensembles phasengleich gekoppelt und generieren simultan Aktionspotentiale mit gleichen Intervallen

(Periodenlängen) und zu gleichen Zeitpunkten (Phasenlage). Verschiedene Ensembles von Neuronen generieren unterschiedliche Periodenlängen und Phasenlagen.

Die Effekte der Applikationen des inhibitorischen Neurotransmitters GABA und des Chloridkanal Blockers Picrotoxin, welcher reproduzierbar GABA-Inhibitionen aufhob, auf die zeitliche Koordination der elektrischen Aktivität, lassen vermuten, dass die neuronalen Ensembles mittels Synchronisation durch GABAerge Interneuronen gebildet werden. Die Phasenlage unterschiedlicher Ensembles wiederum kann durch Applikation von *pigment-dispersing factor* (PDF) synchronisiert werden (das Peptid PDF der Insekten ist homolog zu dem PDH der Crustaceen). Aus den Daten geht hervor, dass diese Phasenkopplung wahrscheinlich aus einer Inhibition der GABAergen Interneurone durch PDF resultiert.

Diese Daten lassen vermuten, dass die Kontrolle der Phasenlage von ultradianen Aktionspotentialoszillationen ein wichtiger Bestandteil der Funktionsweise des circadianen Netzwerks ist.

Offensichtlich wird diese Kontrolle der Phasenlage nicht ausschließlich über chemische Synapsen vermittelt. Die vollständige Blockade der synaptischen Übertragung durch die Entfernung extrazellulären Calciums führte zu einer Erhöhung der elektrischen Aktivität, wahrscheinlich durch den Verlust von inhibitorischen Eingängen auf spontanaktive Zellen, aber nicht zum Verlust von koordinierten Phasenbeziehungen. Die Phasenlage wurde lediglich von null Phasenunterschied zu einer neuen konstanten Phasenbeziehung verschoben.

Kapitel II: Elektrische Synapsen zwischen Neuronen der akzessorischen Medulla scheinen circadiane Schrittmacherzellen der Schabe *Leucophaea maderae* zu synchronisieren

(Gap junctions between accessory medulla neurons appear to synchronize circadian clock cells of the cockroach *Leucophaea maderae*)

Im ersten Kapitel wurde gezeigt, dass GABAerge synaptische Interaktionen zur Bildung neuronalen Ensembles führen. Während alle Neurone eines Ensembles mit der gleichen Phasenlage und gleicher Periodenlänge Aktionspotentiale generieren, zeigen unterschiedliche Ensembles unterschiedliche Periodenlängen und Phasenlagen. Allerdings führt die Blockade von synaptischer Übertragung nicht zu einem völligen Verlust von synchronisierten Aktionspotentialoszillationen, sondern zu einem graduellen Verschieben der Phasenlagen, bis hin zu einem konstanten Phasenunterschied. Daraus lässt sich schließen, dass zusätzliche Synchronisationswege in der aMe eine wichtige Rolle spielen, welche nicht von chemischen Synapsen getragen werden. Um zu untersuchen, ob elektrische Synapsen (*gap junctions*) an dieser Synchronisation beteiligt sind, verwendeten wir die aus Vertebraten bekannten *gap junction* Blocker Halothane, Octanol und Carbenoxolon (CBX). Die Effekte der Applikation von verschiedenen *gap junction* Blockern in Gegenwart und Abwesenheit von synaptischer Übertragung in der aMe, lassen darauf schließen, dass verschiedene Populationen von aMe Interneuronen durch *gap junctions* zu einer stabilen Phasendifferenz synchronisiert werden. Diese Synchronisation schafft die notwendige Voraussetzung für die synaptische Kopplung zu Ensembles von aMe Neuronen mit identischer Phasenlage.

Kapitel III: Extrazelluläre Langzeitableitungen vom circadianen Schrittmacherzentrum der Schabe *Leucophaea maderae* offenbaren circadiane wie auch ultradiane Rhythmen

(Extracellular long-term recordings of the isolated circadian pacemaker center of the cockroach *Leucophaea maderae* reveal circadian as well as ultradian rhythms)

Die elektrische Aktivität der isolierten aMe konnte im Dauerdunkel extrazellulär bis zu fünf Tagen gemessen werden. Bei extrazellulären Saugelektrodenableitungen, wie sie hier durchgeführt wurden ist die gemessene Frequenz unter anderem vom Synchronisationsgrad der einzelnen Neurone abhängig. Hohe Synchronisation zu identischer Phasenlage führt zu einer Verringerung der gemessenen Frequenz und umgekehrt. Da wir zeigen konnten, dass die Synchronisation von Phasenlagen und Periodenlängen ein integraler Bestandteil des aMe Netzwerkes ist, wurde das zeitliche Auftreten von definierten Frequenzmaxima unabhängig von der absoluten gemessenen Frequenz analysiert. Die gemessenen Frequenzmaxima zeigten eine signifikant höhere Verteilung in der Mitte der subjektiven Nacht. Die Untersuchung der Intervallverteilung zwischen den Frequenzmaxima ergab eine vorherrschende ultradiane Periodenlänge von circa zwei Stunden. Zusätzlich traten gehäuft Perioden auf, deren Länge ganzzahlige Vielfache von zwei Stunden waren. Die zeitliche Verteilung dieser periodisch auftretenden Frequenzmaxima, bzw. Frequenzänderungen steht in guter Korrelation zu den Zeiträumen in denen Injektionen von PDF, Allatotropin, GABA und Serotonin die Phasenlage der Lokomotion im Dauerdunkel am stärksten beeinflussen. Es lässt sich vermuten, dass die zeitliche Koordination des aMe Netzwerkes durch die Kontrolle der Phasenbeziehungen ultradianer Oszillatoren bewerkstelligt wird.

Erklärung: Eigene Beiträge und veröffentlichte Teile der Dissertation

Laut Promotionsordnung der Philipps-Universität müssen bei den Teilen der Dissertation, die aus gemeinsamer Forschungsarbeit entstanden, die individuellen Leistungen des Doktoranden deutlich abgrenzbar sein. Dies betrifft Kapitel I-III.

Kapitel I: *Pigment-dispersing factor* und GABA synchronisieren Zellen der isolierten circadianen Uhr der Schabe *Leucophaea maderae*
(Pigment-dispersing factor and GABA synchronize cells of the isolated circadian clock of the cockroach *Leucophaea maderae*)

- Ausarbeitung, Durchführung und Auswertung aller Experimente durch den Autor
- Verfassen der Veröffentlichung in Zusammenarbeit mit Apl. Prof. Dr. Monika Stengl
- Veröffentlichung: Schneider N-L und Stengl 2005, *J Neurosci* 25: 5138-5147. Das vorliegende Kapitel entspricht der Veröffentlichung.

Kapitel II: Elektrische Synapsen zwischen Neuronen der akzessorischen Medulla scheinen circadiane Schrittmacher Zellen der Schabe *Leucophaea maderae* zu synchronisieren
(Gap junctions between accessory medulla neurons appear to synchronize circadian clock cells of the cockroach *Leucophaea maderae*)

- Ausarbeitung, Durchführung und Auswertung aller Experimente durch den Autor
- Verfassen der Veröffentlichung in Zusammenarbeit mit Apl. Prof. Dr. Monika Stengl
- Veröffentlichung: Schneider N-L und Stengl 2005, *J Neurophysiol accepted on Nov. 14, 2005*. Das vorliegende Kapitel entspricht dem akzeptierten Manuskript.

Kapitel III: Extrazelluläre Langzeitableitungen vom circadianen Schrittmacherzentrum der Schabe *Leucophaea maderae* offenbaren circadiane wie auch ultradiane Rhythmen
(Extracellular long-term recordings of the isolated circadian pacemaker center of the cockroach *Leucophaea maderae* reveal circadian as well as ultradian rhythms)

- Ausarbeitung, Durchführung und Auswertung aller Experimente durch den Autor
- Verfassen der Veröffentlichung in Zusammenarbeit mit Apl. Prof. Dr. Monika Stengl
- Veröffentlichung: Schneider N-L und Stengl 2005, *J Neurophysiol submitted on Nov. 23, 2005*. Das vorliegende Kapitel entspricht dem Manuskript.

Introduction

Life on earth has evolved in an environment which is highly periodic in its geophysical parameters. The rotation of the earth around its own axis and the elliptical orbit around the sun cause the 24-hours day with an alternating light-dark cycle and the generation of alternating seasons every year. These temporal rhythms of the environment are reflected in biological rhythms which control almost all behavioral and physiological processes of living organisms directly or indirectly. Biological rhythms are dividable in two categories by the way they are generated. Exogenous biological rhythms are directly driven by environmental or other external cues. Endogenous biological rhythms are not only a simple reaction to environmental rhythms, but they are controlled by endogenous self-sustained oscillators which enable the organisms to anticipate temporal environmental oscillations. These rhythms will be maintained even if the environmental cues remain constant.

General properties of the circadian clock

In the circadian system a self-sustained endogenous pacemaker, the circadian clock, generates oscillations with a period of about 24 hours. Via output pathways the circadian clock then controls the period and the phase of physiological and behavioral rhythms, such as circadian locomotor activity rhythms (Fig. 1). Additionally, the circadian clock is synchronized to environmental rhythms via entrainment pathways. Therefore the endogenous generated period (τ) of the circadian clock can only be determined under constant environmental conditions without any external rhythmic cues (free-running conditions). The period of circadian clocks under free-running conditions (constant darkness) is species-specific and, thus, genetically determined. It is slightly longer than 24 hours in diurnal animals and slightly shorter in nocturnal animals (Aschoff´s rule, Pittendrigh 1960). Additionally, temperature compensation is a vital property of biological clocks. The period lengths of circadian rhythms are almost constant over a wide range of physiological temperatures. This was demonstrated first for eclosion rhythms of *Drosophila* (Pittendrigh 1954) and has been shown in other species including mammals (Menaker 1959; Menaker and Wisner 1983; Underwood 1985; Francis and Coleman 1988; Lee et al. 1990; Zatz et al. 1994).

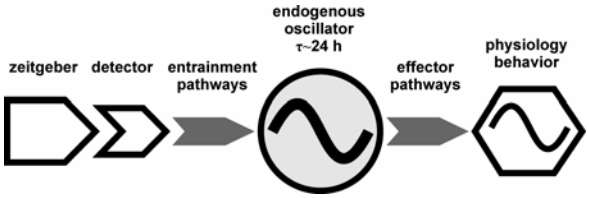

Figure 1: The general model of a circadian clock consists of an endogenous oscillator generating a period of about 24 hours, which is synchronized via entrainment pathways to external rhythms (Zeitgebers). These external rhythms (e.g., rhythmic fluctuations of light, temperature, food supply, or social influences) are detected by appropriate receptors (detector). The clock then controls the temporal organization of physiological and behavioral rhythms (e.g., hormonal rhythms, body temperature, blood pressure, locomotion) via effector pathways.

In order to characterize the time under free-running conditions the circadian time (CT) is used. The free-running period between one phase reference point and the following (e.g., activity onset in behavioral experiments) is divided into 24 circadian hours and defined as the circadian day. In behavioral essays with nocturnal animals the activity onset is a predominant phase reference point and defined as CT 12. Hence, CT 0-12 is the subjective day and CT 12-24 is the subjective night of the animal. The endogenously generated period of the circadian clock slightly differs from 24 hours, therefore it has to be continuously synchronized to external daily rhythms (Zeitgebers). Most important Zeitgebers are the daily cycles of illumination and temperature (Aschoff 1960), but also external rhythms of humidity, food or water availability or social interactions are able to effect the circadian clock. The presentation of various Zeitgebers shifts the phase of the internal clock under free-running conditions in dependence of the phase of the oscillating system. These stimuli can accelerate or delay the circadian oscillator by causing a phase shift (displacement of the rhythm along its time axis).

Phase response curves are obtained by plotting the phase shift against the circadian time when the stimulus was presented. They quantify the effects of Zeitgebers on the phase of a circadian rhythm.

To summarize: Circadian clocks are endogenous self-sustained oscillators, which generate a period of about 24 hours under free-running conditions. They are temperature compensated and the generated period is genetically determined and species specific. Zeitgebers such as environmental rhythms entrain the phase of the circadian clock. Circadian clocks then control the phase and period of physiological and behavioral processes via output pathways.

The molecular clock

The basis for the ability of individual cells to generate self-sustained oscillations is a machinery of interconnected molecular feedback loops and hence called the molecular clock (review by Hardin 2005). The molecules that are involved in the clock function are highly conserved between species, e.g., insects and mammals. "Clock genes" were first described in the fruit fly *Drosophila melanogaster* (Konopka and Benzer 1971), algae (*Clamydomonas reinhardii*, Bruce 1972), fungi (*Neurospora crassa*, Feldman and Hoyle 1973) and much later in mammals (mouse, Vitaterna et al. 1994). In the last years several genes have been shown to be involved in the insect molecular feedback loop of the circadian clock (review by Hardin 2005). The best characterized genes are: *period* (*per*), *timeless* (*tim*), *clock* (*clk*), *cycle* (*cyc*), *vrille* (*vri*), *double-time* (*dbt*), *shaggy* (*sgg*), *par domain protein 1ε* (*pdp1ε*). The products of these genes can be divided by their principal actions within the molecular clocks feedback loop:

Transcriptional activators

The two basic-helix-loop-helix/Pas domain transcription factors, *CLOCK* (*CLK*) and *CYCLE* (*CYK*) form heterodimeres which activate the transcription of *per* and *tim* and the Par domain Protein 1ε (Pdp1ε) which activates the transcription of *clk.*

Transcription repressors

The Pas domain protein *PERIOD* (*PER*) forms heterodimers with *TIMELESS* (*TIM*), which inhibit the function of the *CLK*/*CYK* heterodimer, and *VRILLE* (*VRI*) which represses *CLK* expression.

Proteins which influence translocation

The kinase *SHAGGY* (*SGG*) phosphorylates *TIM* and therefore promotes translocation of *PER/TIM*-heterodimers to the nucleus. The kinase Doubletime (*DBT*) destabilizes *PER*.

In *Drosophila* the molecular circadian oscillator is composed of two interlocked feedback loops in gene expression, the *PER/TIM*-loop and the *CLK* loop (Hardin et al. 1990, 2005; Glossop et al. 1999). The *PER/TIM*-loop is initiated by the binding of CLK/CYK-heterodimers to a regulatory E-box (Darlington et al. 1998; Ritula et al. 1998) and thereby activating the transcription of *per* and *tim* genes. This results in an accumulation of *per*- and *tim*-RNA in the cytoplasm with a peak level in the early night (CT 15), whereas *PER* and *TIM* proteins comprise peak levels in the late evening (CT 19). This delay is a result of phosphorylation dependent destabilization of *PER* by *DBT*, followed by stabilization of phosphorylated *PER* by *TIM* binding (Price et al. 1998; Kloss et al. 1998). *DBT* remains bound to *PER*, resulting in the formation of a *PER*/*TIM*/*DBT*-complex. It is not clear whether the entire complex or possibly *TIM* separately from the *PER*/*DBT*-complex is translocated to the nucleus upon *SGG*-dependent *TIM* phosphorylation (Kloss et al. 2001; Shafer et al. 2002; Ashmore et al. 2003). In the nucleus *PER* remains bound to *DBT*. The phosphorylation of *PER* by *DBT* potentiates the ability of *PER* to interfere with the *CLK*/*CYC*-dimer (Nawathean et al. 2004) and therefore represses the transcription of *per* and *tim* genes (Rothenfluh et al. 2000; Ashmore et al. 2003).

In the *CLK* feedback loop *CLK*/*CYC*-heterodimers bind to E-boxes and activate the

transcription of *vri* and *pdp1ε* (McDonald and Rosbash 2001). The proteins *VRI* and *PDP1ε* have contrary functions. While *PDP1ε* accumulates to high levels during the mid to late evening and activates the transcription of *clk* (Cyran et al. 2003), *VRI* accumulates during late day and early night and inhibits *clk* transcription. These different kinetics of the accumulation of the proteins *VRI* and *PDP1ε* cause an oscillation of *CLK* expression with high *CLK* levels in the late subjective night (Glossop et al. 2003; Cyran et al 2003).

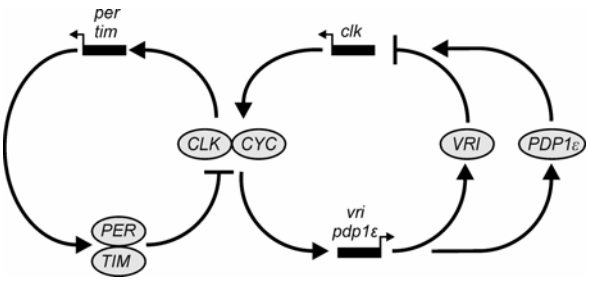

Figure 2: The molecular clock of *Drosophila melanogaster* is composed of two interlocked feedback loops of gene expression. The *CLK*/*CYC*-heterodimer activates the transcription of *per* and *tim*. *PER* and *TIM* proteins form a heterodimer and interfere with the *CLK*/*CYC*-dimer, resulting in an inhibition of *per* and *tim* transcription. The transcription of *clk* is activated by *PDP1ε* and inhibited by *VRI*. The different daily kinetics of the accumulation of the proteins *VRI* and *PDP1ε* cause an oscillation of *CLK* expression with high *CLK* levels in the late subjective night (modified from Stengl 2004).

There are only minor differences in these feed back loops between insects and mammals. The functional analogs of the clock proteins *PER* and *TIM* in the fly are *PER* (*MPER1*, *MPER2* and *MPER3*), and Cryptochrome (*CRY1* and *CRY2*) in the mouse. The transcriptional activators in the fly are *CLK* and *CYC*, in the mouse *BMAL1* is the homolog for *CYC*. Within these striking similarities a fundamental difference concerns the light entrainment of the feedback loops. While light causes the degradation of *TIM* in flies, it induces the transcription of *mper1* and *mper2* genes in the mouse. Therefore light entrainment is established in both species, but via different mechanisms. Additionally, *cyc* expression is not clock controlled in flies, whereas the expression of *mclk* is not clock controlled in mice.

The molecular clock is interconnected with electrical membrane events

The circadian clocks of insects and mammals are composed of different neuronal populations, which exhibit different morphology, physiology, and neurotransmitter content (review by Helfrich-Förster 2004). The central physiological property of neurons is the active regulation of membrane electrical activity. Neuronal membrane events play important roles in the entrainment of circadian rhythms. The accessory medulla (AMe) of *Leucophaea maderae* and the mammalian suprachiasmatic nuclei (SCN) are closely anatomically and morphologically associated with the visual system. In the cockroach the GABA-ir distal tract, the presumptive light entrainment pathway from the compound eyes, arborizes extensively in the noduli of the AMe (Petri et al. 2002; Reischig and Stengl 2003b), while the mammalian retino-hypothalamic tract, originating from a subset of retinal ganglion cells, projects directly into the SCN (Moore 1973; Hatter et al. 2002).

In the cockroach AMe, as in the mammalian SCN, GABA-ir processes are abundant (Van den Pol and Tsujimoto 1985; Moore and Speth 1993; Petri et al. 1995, 2002). In the mammalian SCN it is shown that $GABA_A$-receptor-dependent inhibitions synchronize circadian pacemaker neurons (Strecker et al. 1997; Shinohara et al. 2000; Liu and Reppert 2000; Michel and Colwell 2001). These findings demonstrate the importance of electrical membrane events in the circadian entrainment and expression, but it remains less clear whether electrical activity, postsynaptic events, and transmembrane ion fluxes are also essential features in the circadian rhythm generation. Nitabach et al. (2002) addressed this question in the *Drosophila* circadian system. They found that a constant hyperpolarization of pacemaker neurons` membrane potentials by ectopic expression of K^+-channels stops the free-running oscillation of *PER* and *TIM* in adult *Drosophila* and larvae

(Nitabach et al. 2002, 2005). Therefore they concluded that electrical activity is a necessary component of the cell-autonomous feedback loop that comprise the molecular clock, along with the essential transcription factors and regulatory enzymes that have been identified (Nitabach et al. 2005). This observation can be extended to the mammalian SCN, where hyperpolarization of dispersed SCN cell cultures by decreasing extracellular [K^+] stopped the *PER1* oscillation (Lundkvist 2005).

Circadian rhythms of neuronal activity

Oscillations in the membrane potential causing circadian changes in action potential frequencies of single pacemaker neurons have been described in the mollusc circadian system (Block et al. 1993). In arthropods it is not known if individual pacemaker neurons have the capacity to generate a self-sustained circadian oscillation of electrical activity. But it is shown, that the neuronal network of circadian pacemaker neurons comprises circadian oscillations of electrical activity. Suction electrode recordings of the optical tracts of the optic lobes of the cockroach *Leucophaea maderae* revealed robust circadian rhythmicity in spontaneous electrical activity with peak mean activity during the subjective day (Colwell and Page 1990). In contrast to the cockroach, the circadian rhythm of extracellularly recorded multi-unit activity of the optic lobe of the cricket *Gryllus bimaculatus* comprised maximal mean frequency during the subjective night (Tomioka and Chiba 1992).

From the mammalian SCN it is known that single neurons kept in culture are able to generate circadian rhythms in their electrical activity (Welsh et al. 1995). In vivo recordings with multiunit electrodes revealed high population discharges during the subjective day and low population discharges during the subjective night (Inouye and Kawamura 1982).

The multicellular organization of these bilaterally paired circadian pacemakers by neurons which appear to generate circadian oscillations individually, raises the question how individual cells are coupled to build up a time-keeping system. In the mammalian SCN it is shown that next to hormonal mechanisms, GABAergic interneurons and gap junction mediated coupling play important roles in the synchronization of SCN cells (Jiang et al. 1997; Strecker et al. 1997; Colwell 2000; Liu and Reppert 2000; Shinohara et al. 2000; Michel and Colwell 2001; Schaap et al. 2003; Long et al. 2005).

The accessory medulla: the master clock of the cockroach *Leucophaea maderae*

Lesion and transplantation studies located the circadian clock which controls locomotor activity rhythms of the cockroach *Leucophaea maderae* in the AMe (Stengl and Homberg 1994; Reischig and Stengl 2004). The AMe is a small neuropil in the optic lobes at the anterior, ventromedial border of the medulla and is densely innervated by a manyfold of peptide- and GABA-immunoreactive (-ir) neurons (Homberg et. al. 1991; Petri and Stengl 1995, Petri et al. 2002; Reischig and Stengl 1996). Among the peptid-ir neurons of the AMe are the pigment-dispersing factor-ir (PDF-ir) neurons which are proposed to be circadian pacemaker neurons in the cockroach as well as in the fruitfly (Homberg et al. 1991, 2003; Helfrich-Förster and Homberg 1993; Stengl and Homberg 1994; Helfrich-Förster 1995; Reischig and Stengl 1996, 2004; Sato et al. 2002; Bloch et al. 2003; Sehadová et al. 2003; Závodská et al. 2003). Different AMe compartments are formed by arborizations of peptidergic neurons: the noduli, the internodular, and the shell region (Petri et al. 1995; Reischig and Stengl 1996, 2003b). The noduli and the internodular neuropil are densely innervated by the GABA-ir distal tract which appears to bring light entrainment from the compound eye into the clock. About 25 GABA-ir neurons next to the AMe extensively innervate the AMe neuropil. At least some of them appear to serve as local interneurons.

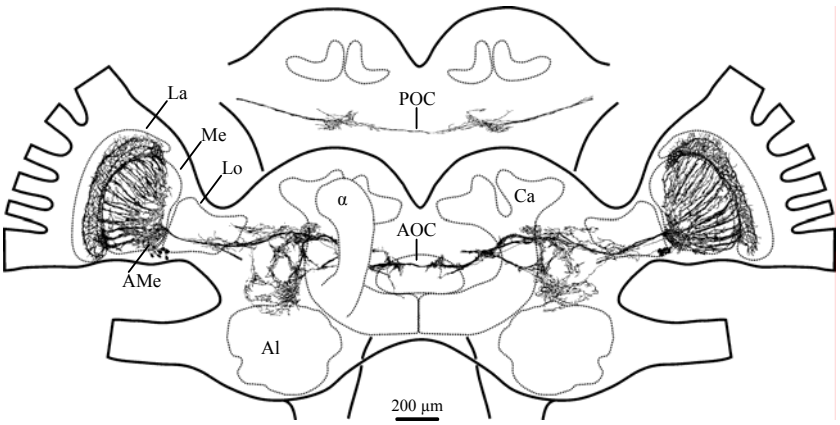

Figure 3: PDF-ir neurons fulfill several morphological criteria predicted for pacemaker neurons. The somata of the PDF-ir neurons are located in the direct vicinity of the AMe with neurites arborizing in the internodular neuropil of the AMe. Some of these neurons send processes into the lamina and project into various areas of the central brain, and form connections to the contralateral optic lobe via the posterior and the anterior optic commissure (POC, AOC). Al: antennal lobe, α: α-lobe, Ca: calyx, La: lamina, Lo: lobula, Me: medulla (modified from Stengl 2004).

The PDF-ir neurons fulfill several morphological criteria predicted for pacemaker neurons. Their somata are located in the direct vicinity of the AMe and they have projections into various areas of the central brain, and connections to the contralateral optic lobe (Homberg et al. 1991, 2003; Stengl and Homberg 1994; Reischig and Stengl 2004). Additionally, PDF-ir processes form both input and output synapses in the AMe, which serve as input and output of the clock (Reischig and Stengl 1996). The PDF-ir neurons, which branch in the internodular neuropil of the AMe, control locomotor rhythms via projections to the superior lateral protocerebrum (Stengl and Homberg 1994; Reischig and Stengl 2003a). In addition, three of the 12 PDF-ir neurons connect both accessory medullae (AMae) and apparently serve to synchronize both pacemakers (Reischig and Stengl 2004). Consistent with this hypothesis, PDF acts as a non-photic input signal into the clock, delaying circadian locomotor activity rhythms (Petri and Stengl 1997). In *Drosophila* PDF is also assumed to be a circadian coupling signal which synchronizes clock cells in the midbrain to control locomotor activity rhythms (Peng et al. 2003; Lin et al. 2004).

The well identified location of the AMe tissue makes it easily accessible for isolation. Furthermore, the well characterized morphology and pharmacology and considerable information gained by behavioral experiments make the AMe of the cockroach an appropriate model for circadian research.

Aims and major findings

While considerable information about the molecular machinery of the core circadian pacemaker is available (Honma and Honma 2003; Hardin 2005), little is known about the clock's physiological properties. It is largely unresolved how circadian coupling in multicellular networks is accomplished and how the neuropeptides act within the clock.

The aim of this doctoral thesis was the electrophysiological and pharmacological characterization of the isolated circadian pacemaker of the cockroach *Leucophaea maderae*, with special focus on the effects of PDF and GABA on the electrical activity of pacemaker neurons. In addition, we addressed the question if the neuronal network of the isolated AMe comprises the capacity to generate a circadian rhythm of electrical activity. Therefore an in vitro essay was established, which enables long-term recordings of multiunit neuronal activity of isolated AMe. For the first time it is possible to investigate and therefore characterize the coordination of electrical activity in the insect circadian neuronal network. Furthermore, it provides insight into the function of neuropeptides and neurotransmitters in the clock`s neuronal network.

Here we show that circadian pacemaker candidates of the AMe of the cockroach produce regular interspike-intervals. Therefore, the cells`

membrane potential oscillates with ultradian periods. Most or all oscillating cells within the AMe are coupled via synaptic and nonsynaptic mechanisms, forming different assemblies. The cells within an assembly share the same ultradian period (= interspike interval) and the same phase (timing of spikes), while cells between assemblies differ in phase. Apparently the majority of these assemblies are formed by inhibitory GABAergic synaptic interactions. Application of pigment-dispersing factor phase-locked and thereby synchronized different assemblies. These data suggest that phase-control of action potential oscillations in the ultradian range is a main task of the circadian pacemaker network.

Interestingly, the recordings revealed that even without synaptic connections all cells remain synchronized and fire with the same frequency at a stable phase relationship. When the extracellular saline is substituted by calcium free saline, which causes disruption of synaptic transmission, more cells become active, apparently due to loss of synaptic inhibitions, but all cells maintain phase coupling and fire very regularly with the same frequency but with a new constant phase difference. After wash out, the cells return to fire with zero phase difference. To determine whether these coupling mechanisms of AMe neurons, which are independent of synaptic release, are based upon electrical synapses between the circadian pacemaker cells, the gap junction blockers halothane, octanol and carbenoxolone were employed in presence and absence of synaptic transmission. We could show that different populations of AMe neurons appear to be coupled via gap junctions to maintain synchrony at a stable phase difference. This synchronization via gap junctions is a prerequisite to phase-locked assembly formation via synaptic interactions and to synchronous gamma-type action potential oscillations within the circadian clock.

In long-term recordings we examined the distribution of activity peaks independently of the absolute action potential frequency. We show that electrical activity peaks are predominantly distributed to the mid-subjective night with a minimum at the middle of the day. Additionally, the analysis of electrical activity peak distribution revealed ultradian periods, that are multiples of a fundamental 2 hours period.

References

Aschoff J. Exogenous and endogenous components in circadian rhythms. In Cold Spring Harbor Symposia on Quantitative Biology: Volume XXV. Biological clocks. New York: Cold Spring Harbor Press. p 11-28, 1960.

Ashmore LJ, Sathyanarayanan S, Silvestre DW, Emerson MM, Schotland P and Sehgal A. Novel insight into the regulation of the timeless protein. *J Neurosci* 23: 7810-7819, 2003.

Bloch G, Solomon SM, Robinson GE, and Fahrbach SE. Patterns of PERIOD and pigment-dispersing hormone immunoreactivity in the brain of the European honeybee *Apis mellifera*: age- and time-related plasticity. *J Comp Neurol* 464: 269-284, 2003.

Block GD, Khalsa SBS, McMahon DG, Michel S, and Geusz M. Biological clocks in the retina: Cellular mechanisms of biological timekeeping. *Int Rev Cytol* 146: 83-144, 1993.

Bruce VG. Mutants of the biological clock in *Chlamydomonas reinhardtii*. *Genetics* 70: 537–548, 1972.

Colwell CS and Page TL. A circadian rhythm in neural activity can be recorded from the central nervous system of the cockroach. *J Comp Physiol A* 166: 643-649, 1990.

Colwell CS. Rhythmic coupling among cells in the suprachiasmatic nucleus. *J Neurobiol* 43: 379-388, 2000.

Cyran SA, Buchsbaum AM, Reddy KL, Lin MC, Glossop NR, Hardin PE, Young MW, Storti RV, and Blau J. vrille Pdp1, and dClock form a second feedback loop in the *Drosophila* circadian clock. *Cell* 112: 329-341, 2003.

Darlington TK, Wager-Smith K, Ceriani MF, Staknis D, Gekakis N, Steeves TD, Weitz CJ, Takahashi JS, and Kay SA. Closing the circadian loop: CLOCK-induced transcription of its own inhibitors per and tim. *Science* 280: 1599-1603, 1998.

Feldman JF and Hoyle MN. Isolation of circadian clock mutants of *Neurospora crassa*. *Genetics* 75: 605–613, 1973.

Francis AJP and Coleman GJ. The effect of ambient temperature cycles upon circadian running

and drinking activity in male and female laboratory rats. *Physiol Behav* 43: 471–477, 1988.

Glossop NR, Houl JH, Zheng H, Ng FS, Dudek SM, and Hardin PE. VRILLE feeds back to control circadian transcription of CLOCK in the *Drosophila* circadian oscillator. *Neuron* 37: 249-261, 2003.

Glossop NR, Lyons LC, and Hrdin PE. Interlocked feedback loops within the *Drosophila* circadian oscillator. *Science* 286: 766-768, 1999.

Hardin PE, Hall JC, and Rosbash M. Feedback of the *Drosophila* period gene product on circadian cycling of its messenger RNA levels. *Nature* 343: 536-540, 1990.

Hardin PE. The circadian timekeeping system of *Drosophila*. *Current Biol* 15: 714-722, 2005.

Hatter S, Liao HW, Takao M, Berson DM, and Yau KW. Melanopsin-containing retinal ganglion cells: architecture, projections, and intrinsic photosensitivity. *Science* 295: 1065-1070, 2002.

Helfrich-Förster C and Homberg U. Pigment-dispersing hormone-immunoreactive neurons in the nervous system of wild-type *Drosophila melanogaster* and of several mutants with altered circadian rhythmicity. *J Comp Neurol* 337: 177-190, 1993.

Helfrich-Förster C. The circadian clock in the brain: a structural and functional comparison between mammals and insects. *J Comp Physiol A* 190: 601-13, 2004.

Helfrich-Förster C. The period clock gene is expressed in central nervous system neurons which also produce a neuropeptide that reveals the projections of circadian pacemaker cells within the brain of *Drosophila melanogaster*. *Proc Natl Acad Sci USA* 92: 612-616, 1995.

Homberg U, Reischig T, and Stengl M. Neural organization of the circadian system of the cockroach *Leucophaea maderae*. *Chronobiol Int* 20: 577-591, 2003.

Homberg U, Würden S, Dircksen H, and Rao KR. Comparative anatomy of pigment-dispersing hormone-immunoreactive neurons in the brain of orthopteroid insects. *Cell Tissue Res* 266: 343-357, 1991.

Honma S and Honma K. The biological clock: Ca^{2+} links the pendulum to the hands. *Trends Neurosci* 26: 650-653, 2003.

Inouye ST and Kawamura H. Characteristics of a circadian pacemaker in the suprachiasmatic nucleus. *J Comp Physiol* 146: 153-160, 1982.

Jiang Z, Yang YQ, and Allen CN. Tracer and electrical coupling of rat suprachiasmatic nucleus neurons. *Neuroscience* 77: 1059-1066, 1997.

Kloss B, Price JL, Saez L, Blau J, Rothenfluh A, Wesley CS, and Young MW. The *Drosophila* clock gene *double-time* encodes a protein closely related to human casein kinase lepsilon. *Cell* 94: 97-107, 1998.

Kloss B, Rothenfluh A, Young MW, and Saez L. Phosphorylation of period is influenced by cycling physical associations of double-time, period, and timeless in the *Drosophila* clock. *Neuron* 30: 699-706, 2001.

Konopka RJ and Benzer S. Clock mutants of *Drosophila melanogaster. Proc Natl Acad Sci USA* 68: 2112-2116, 1971.

Kyriacou CP and Hastings M. Keystone clocks. *Trends Neurosci* 24: 434-435, 2001

Lee TM, Holmes WG and Zucker I. Temperature dependence of circadian rhythms in golden-mantled ground squirrels. *J Biol Rhythms* 5: 25–34, 1990.

Lin Y, Stormo D, and Taghert PH. The neuropeptide pigment-dispersing factor coordinates pacemaker interactions in the *Drosophila* circadian system. *J Neurosci* 24: 7951-7957, 2004.

Liu C and Reppert SM. GABA synchronizes clock cells within the suprachiasmatic circadian clock. *Neuron* 25: 123-128, 2000.

Long MA, Michael JJ, Conners BW, and Burwell RD. Electrical synapses coordinate activity in the suprachiasmatic nucleus. *Nature Neurosci* 8: 61-66, 2005.

Lundkvist GB, Kwak Y, Davis EK, Tei H, and Block GD. A calcium flux is required for circadian rhythm generation in mammalian pacemaker neurons. *J Neurosci* 25: 7682–7686, 2005.

McDonald MJ and Rosbash M. Microarray analysis and organization of circadian gene expression in *Drosophila*. *Cell* 107: 567-578, 2001.

Menaker, M. Endogenous rhythms of body temperature in hibernating bats. *Nature* 184: 1251–1252, 1959**.**

Menaker M and Wisner S. Temperature-compensated circadian clock in the pineal of *Anolis. Proc Natl Acad Sci USA* 80: 6119–6121, 1983.

Michel S and Colwell CS. Cellular communication and coupling within the suprachiasmatic nucleus. *Chronobiol Int* 18: 579-600, 2001.

Moore R and Speth JC. GABA is the principle neurotransmitter of the circadian system. *Neurosci Lett* 150: 112-116, 1993.

Moore RY. Retinohypothalamic projections in mammals: a comparative study. *Brain Res* 49: 403-409, 1973.

Nawathean P and Rosbash M. The doubletime and CKII kinases collaborate to potentiate *Drosophila* PER transcriptional repressor activity. *Mol Cell* 13: 213-223, 2004.

Nitabach MN, Blau J, and Holmes TC. Electrical silencing of *Drosophila* pacemaker neurons stops the

free-running circadian clock. *Cell* 109: 485-495, 2002.

Nitabach MN, Sheeba V, Vera DA, Blau J, and Holmes TC. Membrane electrical excitability is necessary for the free-running larval *Drosophila* circadian clock. *J Neurobiol* 62: 1–13, 2005.

Peng Y, Stoleru D, Levine JD, Hall JC, and Rosbash M. *Drosophila* free-running rhythms require intercellular communication. *PLoS Biol* 1: 32-40, 2003.

Petri B, Stengl M, Würden S, and Homberg U. Immunocytochemical characterization of the accessory medulla in the cockroach *Leucophaea maderae*. *Cell Tissue Res* 282: 3-19, 1995.

Petri B and Stengl M. Pigment-dispersing hormone shifts the phase of the circadian pacemaker of the cockroach *Leucophaea maderae. J Neurosci* 17: 4087-4093, 1997.

Petri B, Homberg U, Loesel R, and Stengl M. Evidence for a role of GABA and Mas-allatotropin in photic entrainment of the circadian clock of the cockroach *Leucophaea maderae. J Exp Biol* 205: 1459-146, 2002.

Pittendrigh CS. On temperature dependence in the clock-system controlling emergence time in *Drosophila*. *Proc Natl Acad Sci USA* 40: 1018–1029, 1954.

Pittendrigh CS. Circadian rhythms and the circadian organization of living systems. In Cold Spring Harbor Symposia on Quantitative Biology: Volume XXV. Biological clocks. New York: Cold Spring Harbor Press. p 159-182, 1960.

Price JL, Blau J, Rothenfluh A, Abodeely M, Kloss B, and Young MW. *double-time* is a novel *Drosophila* clock gene that regulates *PERIOD* protein accumulation. *Cell* 94: 83-95, 1998.

Reischig T and Stengl M. Morphology and pigment-dispersing hormone immunocytochemistry of the accessory medulla, the presumptive circadian pacemaker of the cockroach *Leucophaea maderae*: a light and electronmicroscopic study. *Cell Tissue Res* 285: 306-319, 1996.

Reischig T and Stengl M. Ectopic transplantation of the accessory medulla restores circadian locomotor rhythms in arrhythmic cockroaches (*Leucophaea maderae*). *J Exp Biol* 206: 1877-1886, 2003a.

Reischig T and Stengl M. Ultrastructure of pigment-dispersing hormone-immunoreactive neurons in a three-dimensional model of the accessory medulla of the cockroach *Leucophaea maderae*. *Cell Tissue Res* 314: 421-435, 2003b.

Reischig T and Stengl M. Pigment-dispersing hormone (PDH)-immunoreactive neurons form a direct coupling pathway between the bilaterally symmetric circadian pacemakers of the cockroach *Leucophaea maderae*. *Cell Tissue Res* 318: 553-564, 2004.

Rothenfluh A, Young MW, and Saez L. A TIMELESS-independent function of PERIOD proteins in the *Drosophila* clock. *Neuron* 26: 505-514, 2000.

Rutila JE, Suri V, Le M, So WV, Rosbash M, and Hall JC. CYCLE is a second bHLH-PAS clock protein essential for circadian rhythmicity of *Drosophila* period and timeless. *Cell* 93: 805-814, 1998.

Sato S, Chuman Y, Matsushima A, Tominaga Y, Shimohigashi Y, and Shimohigashi M. A circadian neuropeptide, pigment-dispersing factor-PDF, in the last-summer cicada *Meimuna opalifera*: cDNA cloning and immunocytochemistry. *Zool Sci* 19**:** 821-828, 2002.

Schaap J, Pennartz CMl, and Meijer JH. Electrophysiology of the circadian pacemaker in mammals. *Chronobiol Int* 20: 171-188, 2003.

Sehadová H, Sauman I, and Sehnal F. Immunocytochemical distribution of pigment-dispersing hormone in the cephalic ganglia of polyneopteran insects. *Cell Tissue Res* 312: 113-125, 2003.

Shafer OT, Rosbash M, and Truman JW. Sequential nuclear accumulation of the clock proteins period and timeless in the pacemaker neurons of *Drosophila melanogaster*. J Neurosci 22: 5946-5954, 2002.

Shinohara K, Hiruma H, Funabashi T, and Kimura F. GABAergic modulation of gap junction communication in slice cultures of the rat suprachiasmatic nucleus. *Neuroscience* 96: 591-596, 2000.

Stengl M. Penzlin**,** Lehrbuch der Tierphysiologie: 7. Auflage, 14.5 Biorhythmik. Elsevier Spektrum akademischer Verlag, Germany. 2004.

Stengl M and Homberg U. Pigment-dispersing hormone-immunoreactive neurons in the cockroach *Leucophaea maderae* share properties with circadian pacemaker neurons. *J Comp Physiol A* 175: 203-213, 1994.

Strecker GJ, Wuarin JP, and Dudek FE. $GABA_A$-mediated local synaptic pathways connect neurons in the rat suprachiasmatic nucleus. *J Neurophysiol* 87: 2217-2220, 1997.

Tomioka K. and Chiba Y. Characterization of an optic lobe pacemaker by in situ and in vitro recording of neural activity in the cricket, *Gryllus bimaculatus*. *J Comp Physiol A* 171: 1-7, 1992.

Underwood H. Pineal melatonin rhythms in the lizard *Anolis carolinensis*: effects of light and temperature cycles. *J Comp Physiol* 157: 57–65, 1985.

Van den Pol AN and Tsujimoto KL. Neurotransmitters of the hypothalamic suprachiasmatic nucleus: immunocytochemical analysis of 25 neuronal antigens. *Neuroscience* 15: 1049-1086, 1985.

Vitaterna MH, King DP, Chang A-M, Kornhauser JM, Lowrey PL, McDonald JD, Dove WF, Pinto LH, Turek FW, and Takahashi JS. Mutagenesis and mapping of a mouse gene, Clock, essential for circadian behavior. *Science* 264: 719–725, 1994.

Welsh DK, Logothetis DE, Meister M und Reppert SM. Individual neurons dissociated from rat suprachiasmatic nucleus express independently phased circadian firing rhythms. *Neuron* 14: 697-706, 1995.

Zatz M, Lange GD and Rollag MD. What does changing the temperature do to the melatonin rhythm in cultured chick pineal cells? *Am J Physiol* 266: R50–R58, 1994.

Závodská R, Sauman I, and Sehnal F. Distribution of PER protein, pigment-dispersing hormone, prothoracicotropic hormone, and eclosion hormone in the cephalic nervous system of insects. *J Biol Rhythms* 18: 106-122, 2003.

Cellular/Molecular

Pigment-Dispersing Factor and GABA Synchronize Cells of the Isolated Circadian Clock of the Cockroach *Leucophaea maderae*

Nils-Lasse Schneider and Monika Stengl
Department of Biology, Animal Physiology, Philipps University of Marburg, D-35032 Marburg, Germany

Pigment-dispersing factor-immunoreactive circadian pacemaker cells, which arborize in the accessory medulla, control circadian locomotor activity rhythms in *Drosophila* as well as in the cockroach *Leucophaea maderae* via unknown mechanisms. Here, we show that circadian pacemaker candidates of the accessory medulla of the cockroach produce regular interspike intervals. Therefore, the membrane potential of the cells oscillates with ultradian periods. Most or all oscillating cells within the accessory medulla are coupled via synaptic and nonsynaptic mechanisms, forming different assemblies. The cells within an assembly share the same ultradian period (interspike interval) and the same phase (timing of spikes), whereas cells between assemblies differ in phase. Apparently, the majority of these assemblies are formed by inhibitory GABAergic synaptic interactions. Application of pigment-dispersing factor phase locked and thereby synchronized different assemblies. The data suggest that pigment-dispersing factor inhibits GABAergic interneurons, resulting in disinhibition and phase locking of their postsynaptic cells, which previously belonged to different assemblies. Our data suggest that phase control of action potential oscillations in the ultradian range is a main task of the circadian pacemaker network. We hypothesize that neuropeptide-dependent phase control is used to gate circadian outputs to locomotor control centers.

Key words: **pigment-dispersing factor; circadian pacemakers; ultradian oscillations; circadian clock; GABA; synchronization; resonance**

Introduction

The presence of an endogenous circadian clock in the brain of an animal was demonstrated first in the cockroach *Leucophaea maderae* (Nishiitsutsuji-Uwo and Pittendrigh, 1968; Sokolove, 1975; Page, 1982). However, the cellular basis of the clock remained elusive until pigment-dispersing factor (PDF)-immunoreactive (IR) neurons were proposed as circadian pacemaker candidates in the fruitfly and the cockroach (Homberg et al., 1991, 2003; Helfrich-Förster and Homberg, 1993; Stengl and Homberg, 1994; Helfrich-Förster, 1995). In *Drosophila*, these neurons express clock genes essential for circadian rhythmicity such as *period* and *timeless* (Helfrich-Förster, 1995; Kaneko and Hall, 2000) (for review, see Helfrich-Förster, 2004). The PDF-IR neurons are closely associated with the accessory medulla (AMe), a small neuropil in the optic lobe (Reischig and Stengl, 1996; Sato et al., 2002; Bloch et al., 2003; Sehadová et al., 2003; Závodská et al., 2003), which was identified as the circadian clock of the cockroach (Reischig and Stengl, 2003a). The PDF-IR cells are essential elements of the circadian clock controlling locomotor activity rhythms (Stengl and Homberg, 1994; Reischig and Stengl, 2003a). Associated with the AMe are ~250 cells. More than 60% of these express nuclear PERIOD immunoreactivity (Fischer, 2002).

In the cockroach AMe, as in the mammalian suprachiasmatic nucleus (SCN), GABA-IR processes are abundant (Van den Pol and Tsujimoto, 1985; Moore and Speth, 1993; Petri et al., 1995, 2002). In addition, many different neuropeptide-IR neurons form clock subcompartments, which are dense knots of arborizations (noduli) with looser internodular neuropil and a shell of tracts embracing the AMe (Petri et al., 1995; Reischig and Stengl, 1996, 2003b). Approximately 25 GABA-IR neurons and the GABA-IR distal tract, the presumptive light entrainment pathway from the compound eye, arborize extensively in the noduli of the AMe (Petri et al., 2002; Reischig and Stengl, 2003b). The PDF-IR neurons, which branch in the internodular neuropil, control locomotor rhythms via projections to locomotor control centers in the superior lateral protocerebrum (Stengl and Homberg, 1994; Reischig and Stengl, 2003a). In addition, three of the 12 PDF-IR neurons connect both accessory medullas (AMae) and apparently serve to synchronize both pacemakers (Reischig and Stengl, 2004). Consistent with this hypothesis, PDF acts as a nonphotic input signal into the clock, delaying circadian locomotor activity rhythms (Petri and Stengl, 1997). In *Drosophila*, PDF is also assumed to be a circadian coupling signal that synchronizes clock cells in the midbrain to control locomotor activity rhythms (Peng et al., 2003; Lin et al., 2004).

Received July 15, 2004; revised Feb. 10, 2005; accepted April 4, 2005.

We thank Drs. J. C. Hall (Brandeis University, Waltham, MA) and U. Homberg (Department of Biology, University of Marburg) for helpful revisions of this manuscript and Drs. H. Dircksen and D. Nässel (University of Stockholm, Stockholm, Sweden) for generously supplying PDF peptides. We are thankful for considerable improvement of this manuscript by unknown referees. In addition, we thank Drs. A. Pikovsky and M. Rosenblum (Department of Physics, University of Potsdam, Potsdam, Germany) for helpful discussions of oscillator theory and synchronization of oscillators.

Correspondence should be addressed to Monika Stengl, Department of Biology, Animal Physiology, Philipps University of Marburg, Karl von Frisch Strasse, D-35032 Marburg, Germany. E-mail: stengl@staff.uni-marburg.de.

DOI:10.1523/JNEUROSCI.5138-A-04.2005

 0270-6474/05/255138-10$15.00/0

Although considerable information about the molecular machinery of the core circadian pacemaker is available (Honma and Honma, 2003), little is known about the physiological properties of the clock. It is mostly unresolved how circadian coupling is accomplished and how the neuropeptides act within the clock. Here, we tested in extracellular recordings from excised AMae of the cockroach *L. maderae* whether GABA and PDF affect AMe neurons via modulation of neuronal activity. We discovered that AMe neurons express ultradian action potential oscillations (period-interspike interval) and are grouped into phase-locked assemblies via GABA-dependent synaptic interactions. We hypothesize that PDF-dependent phase locking of assemblies gates clock output to locomotor control centers.

Materials and Methods

All experiments were performed on AMae of adult male cockroaches during the day. Breeding colonies of the cockroach (*L. maderae*) were kept at the University of Marburg at 30°C and 30% humidity in 12 h light/dark cycles, with lights on from 7:00 A.M. to 7:00 P.M. Animals were provided with dry dog food, potatoes, and water *ad libitum*.

The experimental animals were decapitated, and the head capsule was opened to expose the optic lobes. After removal of fat body and the perineurial sheath around the optic lobes, the AMe was excised with a glass pipette (diameter, 150 μm; Flaming/Brown Micropipette Puller, model P-97; Sutter Instruments, Novato, CA). The location of the AMe was easily discernible beneath the bifurcation of a characteristic trachea. All experiments were performed at constant light. Altogether, 32 AMae were used in experiments involving application of GABA and PDF (see below) or of pharmacological agents; additional recordings involved controls (application of vehicle only) and changes of the ionic conditions. In summary, 623 experiments in 32 separate recordings were performed.

For the extracellular recordings, the AMe was transferred to a Petri dish (diameter, 4 cm). All chemicals used were purchased from Sigma-Aldrich (Taufkirchen, Germany). The osmolarity of the extracellular saline (156 mM NaCl, 4 mM KCl, 6 mM $CaCl_2$, 10 mM HEPES, 5 mM glucose, 0.01 g/L phenol red, pH 7.1) was adjusted with mannitol to 380 mOsm. In the Ca^{2+}-free extracellular solution, $CaCl_2$ was replaced by 1 mM EGTA. PDF (NSELINSLLSLPKNMNDA-NH_2), GABA, picrotoxin (PTX), and tetrodotoxin (TTX) were dissolved and diluted in saline. Bicuculline was dissolved in chloroform and diluted in saline. The tissue was continuously superfused with 10 ml of saline per hour at room temperature. Drugs were applied to the tissue either by pressure ejection via glass capillaries (Picospritzer II; General Valve Corporation, Fairfield, NJ) or via bath application to a chamber with a volume of 5 ml and a flow rate of 30–40 ml/h. The doses of applied materials varied according to the following two delivery modes: (1) pressure ejection (PDF, 24–800 fmol; GABA, 1–5 pmol; PTX, 100–200 pmol; bicuculline, 0.4–2 nmol), and (2) bath application (GABA, ranging from 1 to 1000 μM; PTX, ranging from 1 to 1000 μM; bicuculline, 10 μM; TTX, 0.1 μM).

Extracellular electrical activity of the excised AMe was recorded with glass electrodes (0.3–1.5 MΩ) connected to an extracellular amplifier (EXT-01C/DPA 2F; NPI Electronics, Tamm, Germany). Because of the low resistance of the recording electrodes, multiunit action potentials (events) were recorded as upward and/or downward deflections of the baseline. The output of the amplifier was high-pass filtered (3 Hz) to eliminate electrode offset and low-pass filtered (1.5 kHz) to avoid high-frequency noise and aliasing. The signal was digitized (DIGIDATA 1322A; Molecular Devices, Union City, CA) with a sampling rate of 5 kHz and stored on a disk for additional analysis. Event detection via threshold search was performed off-line with SPIKE II software (Cambridge Electronic Design, Cambridge, UK).

The mean frequency (number of events per second) was calculated to evaluate the effects of applied drugs on the firing rate of the cells. Interevent-interval distributions were generated using 1 ms bin width and different periods (depending on the experiment, with a minimum of 100 s) at different time points of the experiment to identify changes in the regularity of the electrical activity. Instantaneous frequency (1/interevent interval) plots were calculated over the whole time course of the experiments to visualize the regularity of electrical activity.

Electrical activity originating from irregularly spiking neurons or from neurons spiking with different rates or phases that are not integer multiples of each other result in a broad cloud of instantaneous frequencies. A defined narrow band of instantaneous frequencies indicates that all recorded cells fire action potentials very regularly at the same or integer multiples of the same interevent interval (harmonic frequencies). Parallel bands in the instantaneous frequency plot indicate that at least two cells fire with the same or integer multiples of the same interevent interval but with different phase relationships. If more than one cell fires with different noninteger multiples of interevent intervals and with different phase, the bands cross each other (Pikovsky et al., 2001). Fusion of parallel bands to one band indicates that the recorded cells now fire with the same phase and the same ultradian period (same interevent intervals). Autocorrelograms were generated using a bin width of 1 ms for an interval of 1 s over

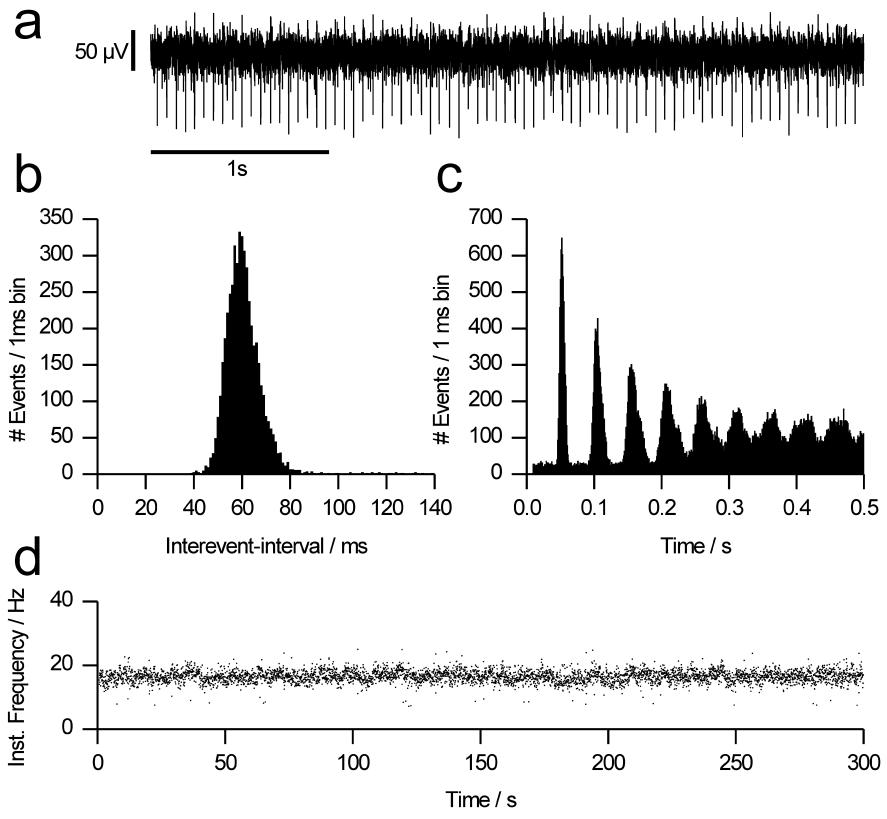

Figure 1. ***a–d***, Neurons of the AMe fire very regularly. ***a***, Extracellular recording from an excised AMe with baseline noise of ~45 μV. The summed action potential activity (events) appears to originate from more than one cell, because it comprises different event amplitudes that occur as downward deflections of the baseline. ***b***, The interevent-interval distribution peaks sharply at ~60 ms, indicating that all recorded cells fire synchronously with the same phase and the same interevent interval. ***c***, Multiple defined peaks in the autocorrelogram show the high regularity of spiking activity of AMe neurons. ***d***, The instantaneous frequency (Inst. Frequency) (1/interevent interval) plot reveals a defined band of ~16.7 Hz.

5–30 min periods to identify rhythmic firing patterns (Groves et al., 1978). Regular interevent intervals cause multiple peaks in the autocorrelogram (Tepper et al., 1995).

Results

In extracellular recordings, we tested whether the neuropeptide PDF and the neurotransmitter GABA affect the electrical activity of interneurons of the AMe of the cockroach *L. maderae*. We show that neurons of the AMe are ultradian oscillators that are grouped into phase-locked assemblies via GABAergic synaptic interactions. PDF transiently phase locked assemblies of neurons apparently via inhibition of GABAergic interneurons, thereby disinhibiting their postsynaptic cells. We hypothesize that this disinhibition activates PDF-IR outputs to locomotor control centers via resonance (see Fig. 9). We assume that circadian clocks are indispensable for phase control of neuronal oscillators also at the time scale of milliseconds, which underlies temporal encoding of the brain.

Extracellular recordings of electrical events of the excised AMe lasted for several hours (Fig. 1). The average peak-to-peak noise amplitude was ~40 μV. Event amplitudes ranged from 50 to 150 μV and were observed as upward and downward deflections from the baseline, depending on the impedance ratio between the recorded neurons, the recording electrode, and the indifferent electrode. Application of the sodium channel blocker TTX (10^{-8} M) reversibly blocked all electrical events within several hours after application to the bath solution (data not shown; $n = 3$ experiments in three different preparations).

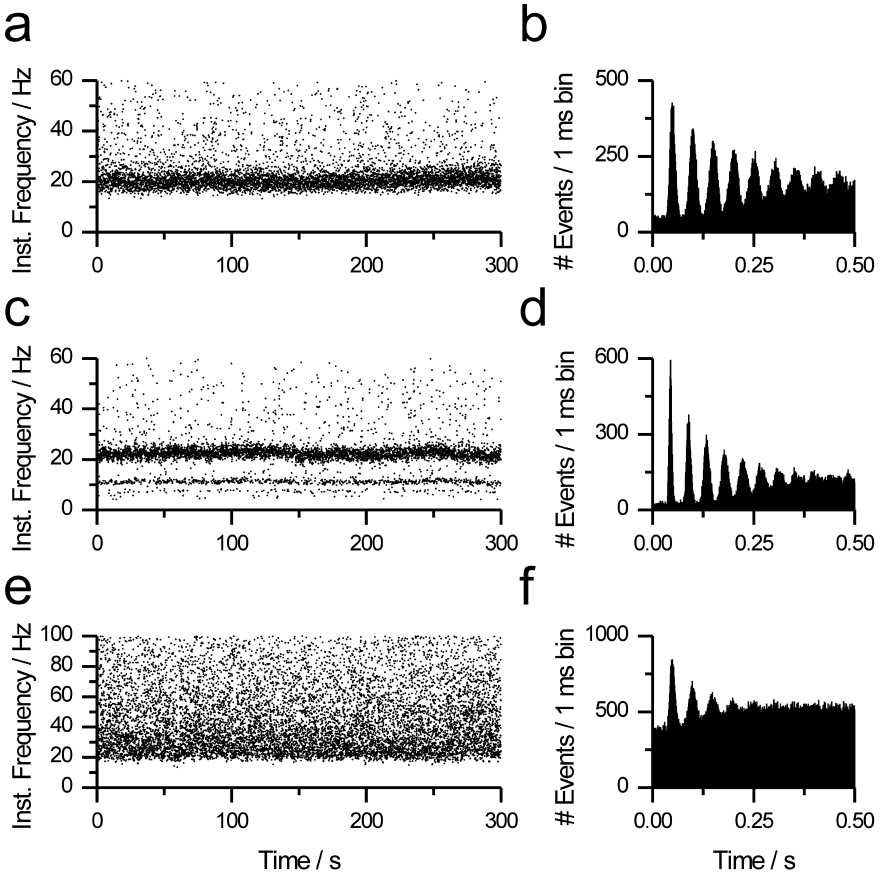

Figure 2. ***a–f***, Instantaneous frequency (Inst. Frequency) plots reveal that AMe neurons fire regularly at the same or at different phases. ***a***, One narrow band in the instantaneous frequency plot indicates that cells fire with the same phase and the same or integer multiples of the same interevent interval. ***b***, The regular interevent intervals result in multiple peaks in the autocorrelation. ***c***, Cells spiking with the same or integer multiples of the same interevent interval but with different phase show several distinct bands in the instantaneous frequency plot. ***d***, The multiple peaks in the autocorrelation analysis are indicative of oscillatory spiking activity. ***e***, If cells spike with the same or integer multiples of the same interevent interval but with many different phase relationships, the instantaneous frequency plots do not show regularity. ***f***, Autocorrelation analysis, however, still reveals regularity in the spiking pattern.

Extracellular recordings usually were multiunit recordings and were composed of activity from more than one cell with different event amplitudes (Fig. 1*a*). Less than five recordings appeared to result from single cells. These showed constant action potential amplitude and regular firing pattern, which resulted in a sharp peak of the interevent-interval histogram (data not shown for single cells) (Fig. 1*b*, multiunit recording). Likewise, >80% of the multiunit recordings (of 32 preparations) showed sharp multiple peaks in the autocorrelograms, indicating regular firing modes of recorded neurons (Tepper et al., 1995) (Figs. 1*c*, 2*b*,*d*,*f*).

In 72% of all recordings, spontaneous activity occurred in one to seven parallel bands in the instantaneous frequency plot (1/interevent interval; see Materials and Methods). Activity in one band originates from spontaneously active cells that fire at the same phase and the same or integer multiples of the same interspike interval (harmonic frequencies) (Figs. 1*d*, 2*a*). Parallel bands indicate that neurons with the same or with integer multiples of the same frequency fire with a stable phase difference (Figs. 2*c*, 3*c*) (see Figs. 5*c*, 7*c*, 8*c*). Thus, spontaneously active ultradian oscillators are grouped into assemblies. All cells within an assembly fire phase locked with the same or with harmonic frequencies, whereas cells between assemblies fire at a stable phase difference.

To examine whether the regular action potential activity of AMe neurons is a property of the single cells or whether it is caused by synaptic synchronization of irregularly spiking neurons, we superfused the AMe with Ca^{2+}-free or high Mg^{2+} saline to inhibit neurotransmitter release (Fig. 3). Application of Ca^{2+}-free saline resulted in an increase of the mean event frequency and amplitude, apparently as a result of release from synaptic inhibition. In 19 of 23 experiments (involving 13 preparations), the sharp band of instantaneous frequencies broadened and gradually increased to a higher frequency level. Simultaneously, several new bands of lower frequency appeared parallel to the high-frequency band. Thus, the previously single assembly split into different assemblies. Superfusion with saline containing 10 mM Mg^{+2} mimicked the effects of low-divalent solutions ($n = 3$) (data not shown), suggesting that the observed changes in activity are caused by loss of synaptic connections and not only by changes in the extracellular Ca^{2+} concentration.

Several events appear to underlie these observed phenomena. Neurons of one assembly, firing in synchrony with the same phase, appear to gradually shift to a new constant phase while

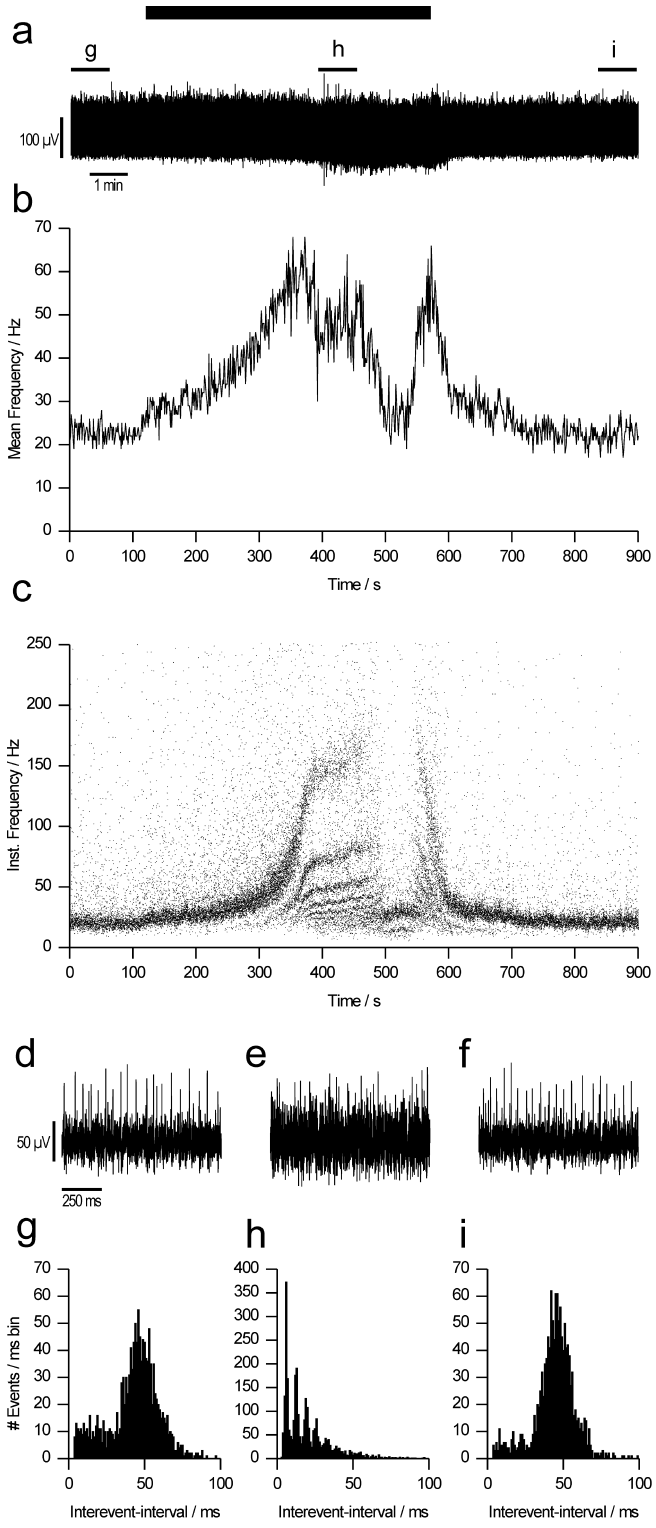

Figure 3. ***a–i***, Regular spiking AMe neurons are synchronized to the same phase and frequency by inhibitory synaptic interactions. ***a***, The black bar indicates the substitution of extracellular saline for Ca^{2+}-free solution to disrupt synaptic activity in the extracellular recording of the excised AMe. The same time axis is used in ***a–c***. Thin bars (g, h, i) indicate the time window for the interevent-interval distributions in ***g–i***. The Ca^{2+}-free solution causes a larger variability of event amplitudes and a rise in the mean frequency (***b***), apparently resulting from disinhibition and shift of phase as seen in ***c***. The instantaneous frequency (Inst. Frequency) plot (***c***) and the interevent-interval distributions (***g–i***) illustrate that, in normal saline, all cells fire in synchrony at the same phase and a lower action potential frequency. After disruption of synaptic activity, the sharp 22.7 Hz band continuously increases to a higher instantaneous frequency while new parallel bands appear. Thus, without synaptic contacts, more cells become active, but all cells maintain coupling and fire very regularly with the same or integer multiples of the same interevent interval but with a constant phase difference (***h***). The sudden, reversible inhibition at 500 s in ***c*** occurred spontaneously, possibly resulting from store-dependent Ca^{2+} release. ***d–f***, Original trace at an expanded time scale (at time points g, h, and i in ***a***).

increasing their firing frequency. In addition, previously silent neurons appear to discharge action potentials but at the same interspike interval and with constant phase relationship to the firing neurons. Thus, without synaptic communication, cells remained coupled ultradian oscillators but split into different assemblies that fired with constant phase difference and with higher frequency. After returning to extracellular saline with 6 mM Ca^{2+} concentrations, the parallel bands smoothly declined and fused to one lower frequency band ($n = 10$). These findings indicate that all cells gradually returned to firing in synchrony. Apparently, via inhibitory synaptic interactions again, they formed an assembly and fired at the same phase and at the same lower frequency (Fig. 3*c*). Frequently, a sharp drop in instantaneous frequency occurred when we switched back to high-Ca^{2+}-containing extracellular saline but before complete exchange of the low-divalent extracellular solution. It is possible that this sudden inhibition of activity is caused by sudden synchronous release of an inhibitory neurotransmitter either via Ca^{2+} release from intracellular stores or via Ca^{2+} influx.

Dense GABA immunostaining in the AMe (Petri et al., 2002) suggests that GABA essentially is responsible for the inhibitory synaptic interactions between AMe neurons. Application of GABA (1–5 pmol via picospritzer; 1 μM to 1 mM via bath) resulted in a dose-dependent strong inhibition of electrical activity (Fig. 4) in 98% of all experiments ($n = 453$; 15 preparations). Reduced spiking activity developed within 1 to 2 s after application. Activity returned within 10 to 100 s, depending on the applied dose. In approximately one-third of all experiments in instantaneous frequency plots, GABA-dependent phase locking of cells was observed before electrical activity ceased (data not shown). Application of the vertebrate $GABA_A$ receptor antagonist bicuculline (0.4–2 nmol) showed no effect ($n = 5$; five preparations). Because bicuculline is also without effect on $GABA_A$ receptors in other invertebrate preparations, whereas the chloride channel blocker picrotoxin was used successfully as a GABA channel antagonist (Lee et al., 2003; Sattelle et al., 2003), we used picrotoxin. Picrotoxin (1 μM to 1 mM) reproducibly opposed GABA-dependent inhibition. Picrotoxin application increased electrical activity, the instantaneous frequency band smoothly increased, and several parallel bands appeared. Thus, in the presence of picrotoxin, cells split into different assemblies and remained synchronized but resumed a stable phase difference and fired with higher frequencies ($n = 6$; five preparations) (Fig. 5). The density of the bands increased after picrotoxin application and smoothly shifted to higher instantaneous frequencies. This indicates that previously silent cells gradually started to fire. However, these neurons always remained phase locked at a stable phase difference, because several parallel bands appeared, not just noise, or only one band at a higher instantaneous frequency. Because picrotoxin is not specific for GABA receptors but blocks different chloride channels, we cannot exclude that it might also inhibit other ligand-gated chloride channels such as glutamate receptors.

Application of PDF (24–800 fmol with picospritzer) during the day (Zeitgebertime ZT 4–11) changed the electrical activity of AMe neurons in 78% of all experiments. Peptide application ei-

←

ther transiently decreased ($n = 58$; seven preparations) or increased ($n = 76$; four preparations) neuronal activity after delays of 1–100 s (Fig. 6). In low-divalent solutions, which disrupt synaptic transmission, PDF always led to neuronal inhibition ($n = 5$, involving three preparations) (Table 1), suggesting that the excitatory effects in normal saline were indirect effects through inhibitory interneurons. Indeed, after PDF-induced transient activations, removal of extracellular Ca^{2+} or elevation of Mg^{2+} abolished the PDF effect ($n = 7$; three preparations). In the presence of picrotoxin (Table 1), in two experiments, PDF-dependent activation was seen ($n = 2$; one preparation) whereas in 11 experiments, PDF-dependent inhibition was observed ($n = 11$; one preparation). Thus, PDF-dependent inhibition/disinhibition appears not to be mediated via chloride channel opening. PDF-dependent increases in the event amplitudes (Figs. 6*a*, 7*a*) were observed, which resulted from either disinhibition of previously inhibited cells or PDF-dependent synchronization of cells, which were not phase locked previously to the same phase. High-amplitude events were abruptly and transiently elicited superimposed on the background activity accompanied by an increase in the mean frequency (Fig. 6*a*); thus, PDF disinhibited new units. In other recordings, the event amplitudes increased gradually while the mean frequency decreased (Figs. 7*a*,*b*). These PDF-dependent increases in the event amplitudes resulted from synchronization of units, which previously belonged to different assemblies, as shown in instantaneous frequency plots (Fig. 7*c*).

In recordings with several instantaneous frequency bands, PDF caused a transient, smooth fusion of the bands to a higher synchronized instantaneous frequency compared with the lowest frequency band before application but to a lower instantaneous frequency compared with the highest band before application (Fig. 7). Because the previously parallel bands are fused to one dense band, PDF strictly synchronizes and phase locks the recorded units to the same phase (Fig. 7*c*). Because after PDF application the fused band maintains a higher instantaneous frequency than the lowest frequency band before application, PDF disinhibited AMe neurons ($n = 16$; five preparations) (Fig. 7). At the same time, PDF inhibited previously active cells, because the fused band maintains a lower synchronized instantaneous frequency compared with the highest frequency band before application.

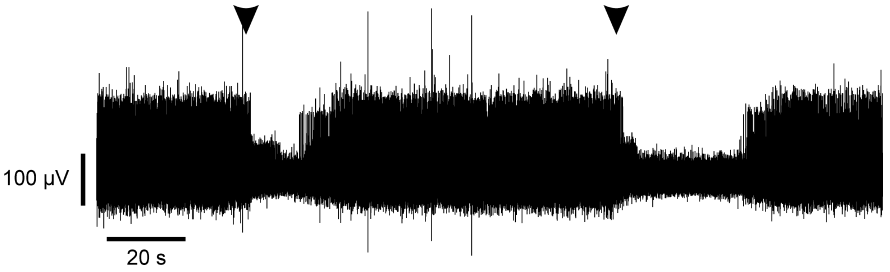

Figure 4. The neurotransmitter GABA inhibits AMe neurons dose dependently. Application of 0.1 pmol of GABA (left arrowhead) and 0.5 pmol of GABA (right arrowhead) inhibits electrical activity of the AMe neurons with different durations.

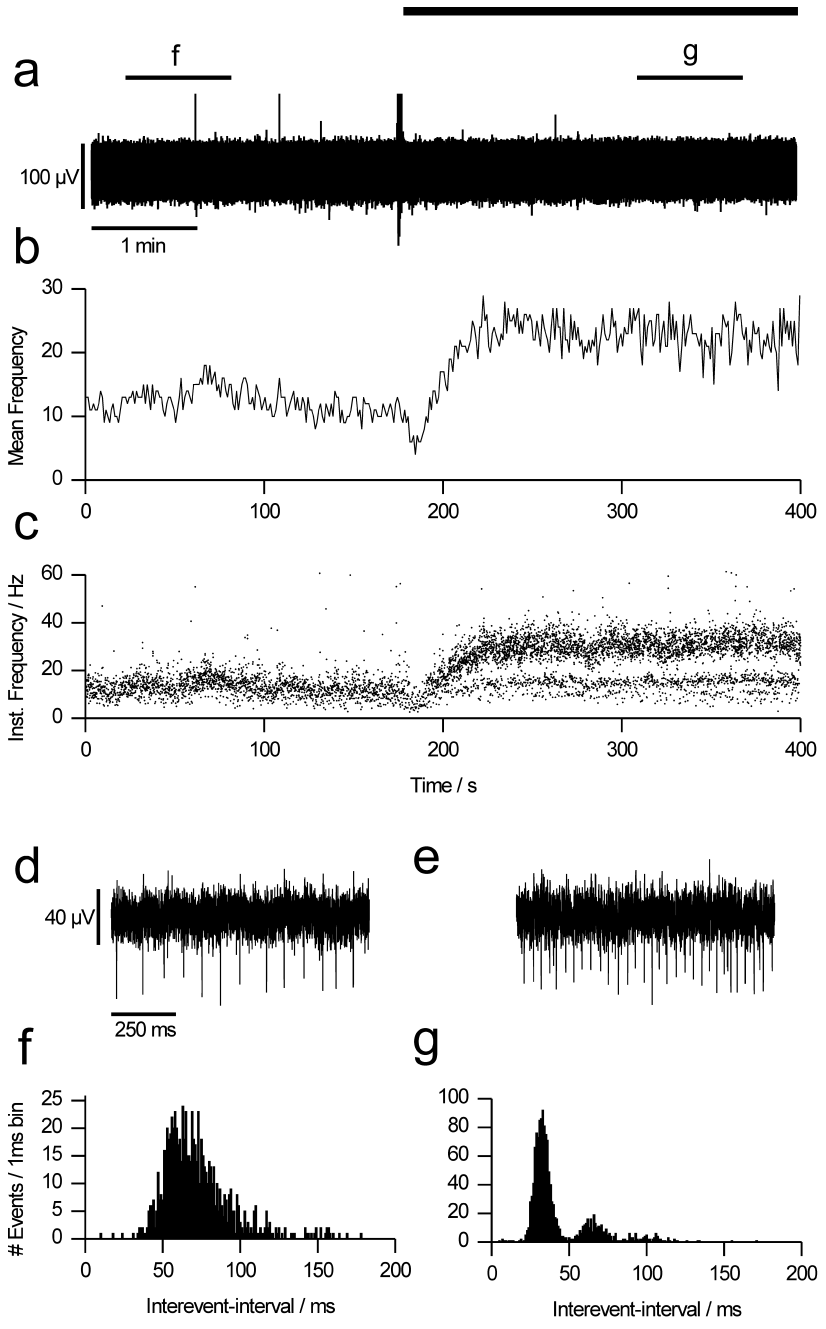

Figure 5. In the presence of the Cl^- channel antagonist picrotoxin (which also blocks $GABA_A$ receptors), AMe neurons remain synchronized but fire with a stable phase difference and a higher frequency. ***a***, Original recording trace over 400 s. The black bar marks bath application of 1 mM picrotoxin. Thin bars (f, g) indicate the time frames of interevent-interval distributions in ***f*** and ***g***. ***c***, The instantaneous frequency (Inst. Frequency) plot shows phase desynchronization of AMe neurons during picrotoxin application. ***d***, ***e***, Original trace at an expanded time scale (at time points f and g in ***a***). ***f***, ***g***, The interevent-interval distributions show that, before and during picrotoxin application, the AMe neurons maintain regular firing activity.

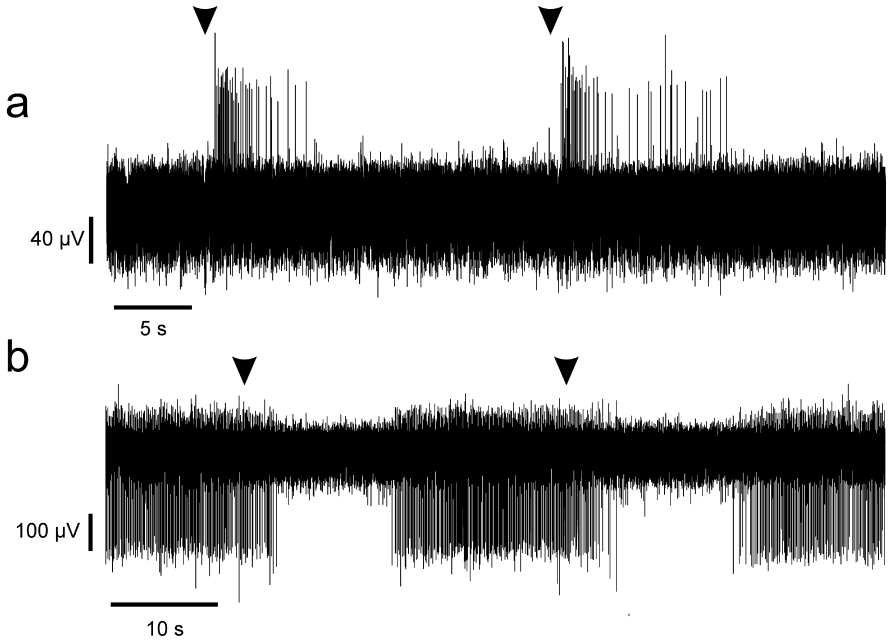

Figure 6. PDF leads to activation or inhibition of AMe neurons. ***a***, After PDF application of 75 fmol (arrowheads), large events appeared superimposed on the background activity (***b***). In another recording, 75 fmol PDF inhibited AMe neurons, repetitively.

Table 1. Effects of PDF application to excised accessory medullas of the cockroach *L. maderae* in different extracellular salines

Saline	Ca^{2+}-free saline	Saline plus picrotoxin	
Activation	No effect	Not tested	$n = 7$ (3 preparations)
Activation	Not tested	Activation	$n = 2$ (1 preparation)
Inhibition	Inhibition	Not tested	$n = 5$ (3 preparations)
Inhibition	Not tested	Inhibition	$n = 11$ (1 preparation)

During the fusion of the bands, the event amplitudes in the original recordings transiently increased (by ~20%) (Fig. 7*a*) while the mean frequency dropped. This effect of PDF application indicates superposition of action potentials of different cells, which now fire at the same phase and the same or integer multiples of the same interevent intervals. In addition, the mean frequency increased while the peptide-dependent fusion of the instantaneous frequency bands gradually disappeared. This particular result suggests that during washout (because of perfusion of the dish) of PDF, the phases of the neurons smoothly drifted apart again until their previous stable frequency and phase relationships were restored. The smoothness of transitions from parallel bands to one fused band and back to parallel bands indicates that the recorded AMe neurons always remained synchronized. Thus, PDF only synchronized the phase of perpetually coupled AMe neurons, which previously belonged to different assemblies. Control applications of vehicle resulted in none of the physiological modulations as described for the PDF effects (Fig. 8) ($n = 9$; five preparations).

Discussion

Extracellular recordings from the excised AMe, the circadian clock of the cockroach *L. maderae*, investigated the function of PDF and of GABA on neuronal spike discharges. Circadian pacemaker candidates fire action potentials with regular interspike intervals and are coupled via synaptic and nonsynaptic mechanisms. They are organized into phase-locked assemblies via GABAergic interneurons. Different assemblies distinguished by a stable phase difference were transiently synchronized to the same phase and period by PDF. We assume that PDF-dependent phase locking activates outputs to locomotor control centers (Fig. 9).

AMe neurons are synchronized by GABA

Picrotoxin application caused a pronounced increase of the instantaneous frequency, together with the appearance of new parallel instantaneous frequency bands. This suggests that Cl^- channel-dependent inhibitory synaptic transmission synchronizes the phase of AMe neurons. Because GABA immunoreactivity is prominent in the AMe and because, in most of our recordings, GABA inhibited neuronal activity, the majority of inhibitory connections appear to be mediated via $GABA_A$ receptors. Because picrotoxin is not specific for $GABA_A$ receptors, we cannot exclude that other inhibitory neurotransmitters are also involved.

The occurrence of several parallel bands in instantaneous frequency plots indicates that different phase-locked assemblies of AMe neurons fire at a constant phase difference. Because picrotoxin further split and multiplied parallel bands while GABA fused them, GABAergic interneurons appear to form different neuronal assemblies within the AMe, keeping cells within an assembly synchronized and phase locked to the same phase (below or above spiking threshold). A similar self-organization into phase-locked assemblies with stable phase differences was demonstrated in computer simulations for coupled oscillators (Klevecz at al., 1984, 1991; Kunz and Achermann, 2003).

In the mammalian SCN, GABA is the predominant neurotransmitter (Moore and Speth, 1993; Wagner et al., 1997; De Jeu and Pennartz, 2002) and has been shown to synchronize circadian pacemaker neurons via $GABA_A$ receptor-dependent inhibitions (Strecker et al., 1997; Liu and Reppert, 2000; Shinohara et al., 2000; Michel and Colwell, 2001). Synchronization of neurons via GABAergic interneurons is also used in other parts of the insect brain such as the antennal lobe, in which neuronal synchronization appears to be important for odor coding (Christensen et al., 2000; Laurent, 2002).

AMe neurons show sharp parallel bands in the instantaneous frequency plots even after disruption of synaptic connections, which indicates that they are still synchronized but now maintain a stable phase difference. Therefore, there must be additional, nonsynaptic interactions between the AMe neurons such as gap junctions, glia-neuron interactions, or nonsynaptic release of neuromediators (Shinohara et al., 1995; Jiang et al., 1997; Tamada et al., 1998; Michel and Colwell, 2001; Cheng et al., 2002; Schaap et al., 2003). We are currently testing with dye injections as well as pharmacologically whether gap junctions couple AMe neurons. Whether the multitude of different peptides that occur in the circadian clock of *L. maderae* might contribute to nonsynaptic synchronization remains to be examined (Petri et al., 1995).

AMe neurons are synchronized by PDF

In *L. maderae*, the 12 PDF-IR neurons of the AMe apparently serve in different circuits of the circadian clock (Reischig and Stengl, 2002, 2003a,b, 2004). The small, weakly staining PDF-IR neurons appear to be local neurons of the AMe; two large and one medium PDF-IR neurons directly connect both AMae, whereas the other large and medium cells form outputs to various midbrain and optic lobe targets (Reischig and Stengl, 2004). Thus, in *L. maderae*, as in *Drosophila*, PDF-IR neurons are circadian pacemaker candidates and, at the same time, serve as nonphotic clock inputs and outputs. Their peptide PDF is assumed to synchronize the bilaterally symmetric clocks, the pacemaker cells within one AMe, and apparently postsynaptic pacemakers in the midbrain (Helfrich-Förster et al., 1998; Homberg et al., 2003; Lin et al., 2004).

Drosophila mutants without PDF lose circadian locomotor activity rhythms in constant darkness (Renn et al., 1999), whereas ectopic expression of PDF causes highly increased irregular activity. This indicates that PDF regulates locomotor activity rhythms in *Drosophila* (Helfrich-Förster et al., 2000). In the cockroach, lesion and transplantation experiments showed that PDF-IR neurons with projections to the superior medium protocerebrum are necessary and sufficient for the control of locomotor activity rhythms (Stengl and Homberg, 1994; Reischig and Stengl, 2003a). In addition, PDF injections into the vicinity of the AMe delayed the onset of locomotor activity rhythms during the late day, indicating that PDF action in the AMe affects clock outputs (Petri and Stengl, 1997). Furthermore, in *Drosophila*, PDF-dependent communication among clusters of neurons in the dorsal brain that contain clock-gene products seems to be necessary for maintaining the phase and amplitude of clock gene expression rhythms and for sustaining circadian activity rhythms (Peng et al., 2003; Lin et al., 2004). Thus, in the fruitfly as well as in the cockroach, PDF is assumed to be an output signal of the clock to midbrain oscillators controlling onset of locomotor activity rhythms.

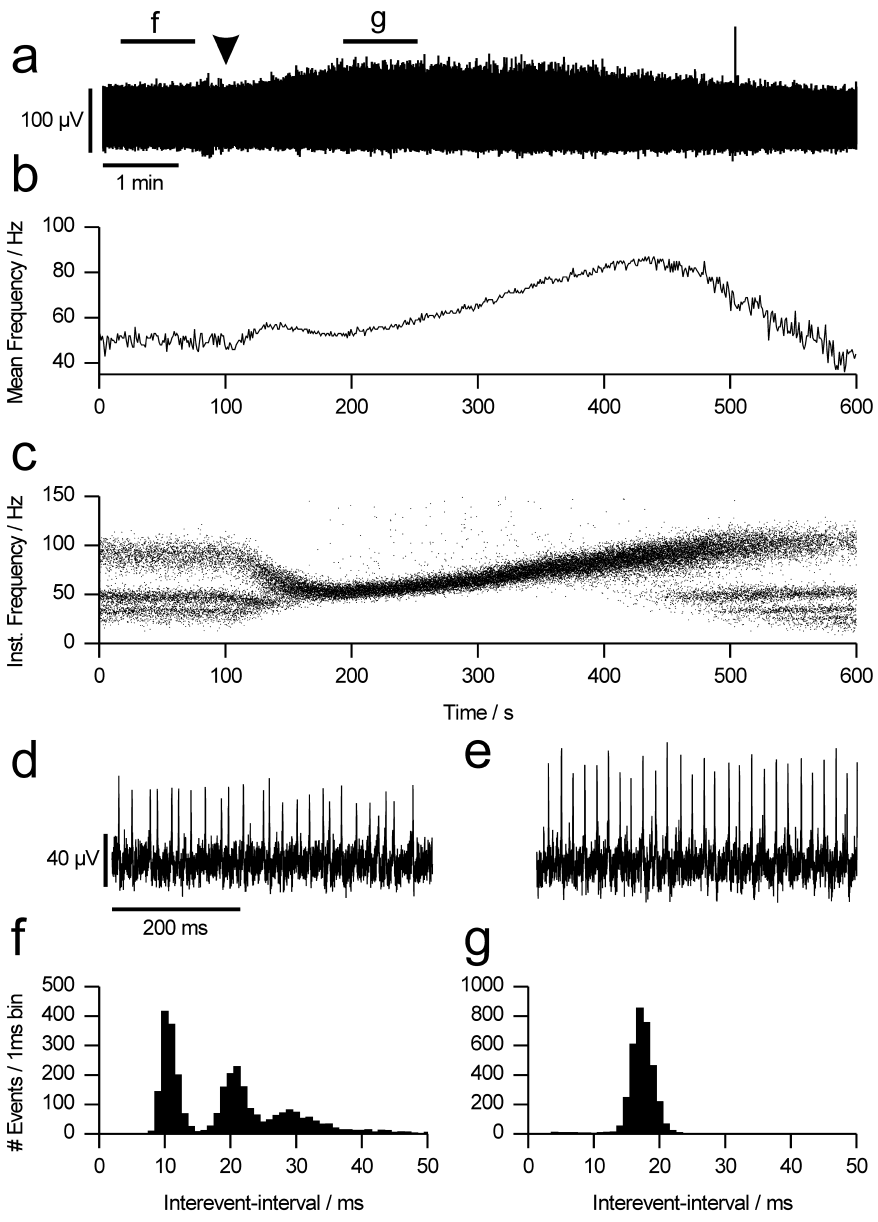

Figure 7. PDF synchronizes AMe neurons. ***a***, After application of 75 fmol PDF (arrowhead), the event amplitudes increased continuously and transiently. Bars (f, g) indicate where interevent-interval distributions were calculated. ***b***, After PDF application, there is a small transient increase in the mean frequency, followed by a transient decrease to a level that is higher than the starting level. Then, a continuous stronger rise occurs before the mean frequency declines again to a level below the starting level. Comparison with ***c*** shows that rises in the mean frequency correlate with desynchronization, whereas the declines correlate with synchronization of spiking neurons. ***c***, The parallel, distinct bands in the instantaneous frequency (Inst. Frequency) plot indicate that at least two AMe neurons fire synchronized with the same (or at integer multiples of the same) interevent interval but at a different phase. Application of PDF synchronizes and phase locks the neurons transiently; thus, now all cells fire at the same time with the same frequency as seen in the superposition of amplitudes (compare ***d***, ***e***) and the single peak in the interevent interval distribution (***g***). The interevent-interval distribution (***f***) shows that at least two regularly firing synchronized cells (or assemblies of cells) with a constant phase difference are hidden in the apparently irregularly occurring events of the original recording (***d***). In ***e*** and ***g***, the cells are now phase locked to the same phase, and their event amplitudes superimpose.

Here, we show that PDF synchronized cells to the same phase with smooth phase shifts while decreasing and/or increasing their ultradian periods (interspike intervals). Apparently, PDF acts as an inhibitory peptide, because in the absence of synaptic connections, PDF only inhibited but never activated neurons. Therefore, the observed PDF-dependent activations most likely result from inhibition of inhibitory interneurons. Because PDF-dependent disinhibitions were observed in the presence of picrotoxin, in addition to GABAergic interneurons, other inhibitory interneurons appear to have PDF receptors. Thus, our data suggest that synchronization of circadian clock cells within the AMe, between both AMae, and between the clock and postsynaptic oscillators is accomplished by phase locking action potential oscillations. PDF-dependent disinhibition might also gate the coupling pathway to the contralateral pacemaker center, which synchronizes both AMae. In addition, it is possible that PDF-dependent phase locking of clock cells with

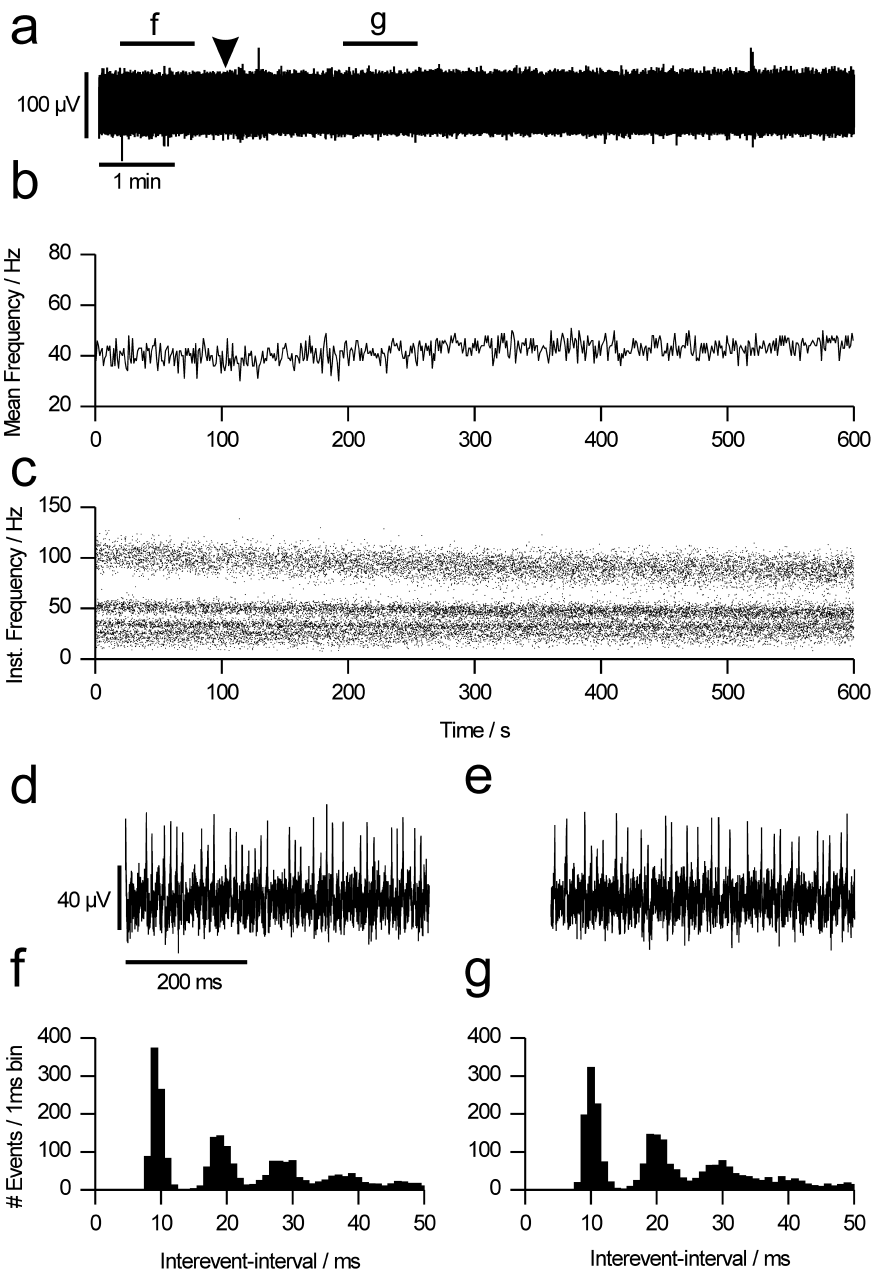

Figure 8. Control applications of vehicle do not affect AMe neurons. No vehicle-dependent changes are seen in the original recording (***a***), the mean frequency plot (***b***), the instantaneous frequency (Inst. Frequency) plot (***c***), or the interevent-interval distributions (***f***, ***g***). ***d***, ***e***, Original trace at an expanded time scale (at time points f and g in ***a***).

PDF-IR output pathways via the anterior optic commissure to the superior medium protocerebrum (Reischig and Stengl, 2003a) might gate the onset of circadian locomotor activity during late day.

AMe neurons generate ultradian action potential oscillations

Our experiments show for the first time that the large majority of neurons of the AMe fire very regularly. Because this regular spiking activity is maintained in the absence of synaptic interactions, it is likely that the discharges are generated endogenously. It is possible that the membrane potential of circadian pacemaker candidates oscillates endogenously and thereby elicits action potentials in regular interspike intervals. Regular oscillations in the membrane potential causing circadian changes in action potential frequencies have also been described in mollusc circadian pacemaker cells (Jacklet, 1988; Block et al., 1995), but it was not analyzed whether all of these also fire regularly on an ultradian scale. Whether all regularly discharging cells of the cockroach circadian clock are also endogenous circadian pacemaker neurons and vice versa remains to be examined. PDF-IR neurons apparently generate very regular interspike intervals, because intracellular recordings from neurons with the same branching pattern as PDF-IR neurons showed spontaneous discharge rates with regularly spaced spikes (Loesel and Homberg, 2001). In addition, regularly bursting neurons with arborizations in the circadian clock were recorded (Loesel and Homberg, 1998, 2001). The importance of the membrane potential for circadian oscillations is also suggested by Nitabach et al. (2002), who showed that constant hyperpolarization of the membrane of circadian pacemaker neurons in *Drosophila* interrupts circadian oscillations in clock gene expression in the nucleus. In the nucleus, clock gene products such as PERIOD and TIMELESS suppress their own transcription via a negative-feedback loop. Several interlocked feedback loops of different clock genes generate 24 h rhythms in their mRNA and protein levels (for review, see Honma and Honma, 2003). Thus, it is likely that the observed ultradian action potential rhythms and the molecular feedback loop in the nucleus are intimately connected. In the SCN of mammals, circadian pacemaker candidates with regular interevent intervals have also been observed, but the relevance of these ultradian oscillations for circadian rhythms remained unresolved (Gross and Hendriks, 1979; Shibata et al., 1984; Cahill and Menaker, 1989; Pennartz et al., 1998; Schaap et al., 1999).

Because the majority of AMe neurons fired regularly, our experiments indicate that ultradian membrane oscillations might be an important property of circadian pacemaker neurons, possibly leading to circadian scale oscillations via high-frequency oscillator coupling (Klevecz et al., 1984, 1991). Because information processing in the brain happens at the time course of milliseconds, circadian oscillators, which precisely effect timing of different physiological processes at different phases, should also be precise at the time course of milliseconds and seconds and not only at the time course of hours.

Information processing between phase-locked ultradian oscillators as presynaptic and postsynaptic cells is precise, fast, and happens with improved signal-to-noise ratio as the cells resonate, a mechanism of temporal encoding widely used in the mammalian brain (Izhikevich et al., 2003). Resonance occurs if the

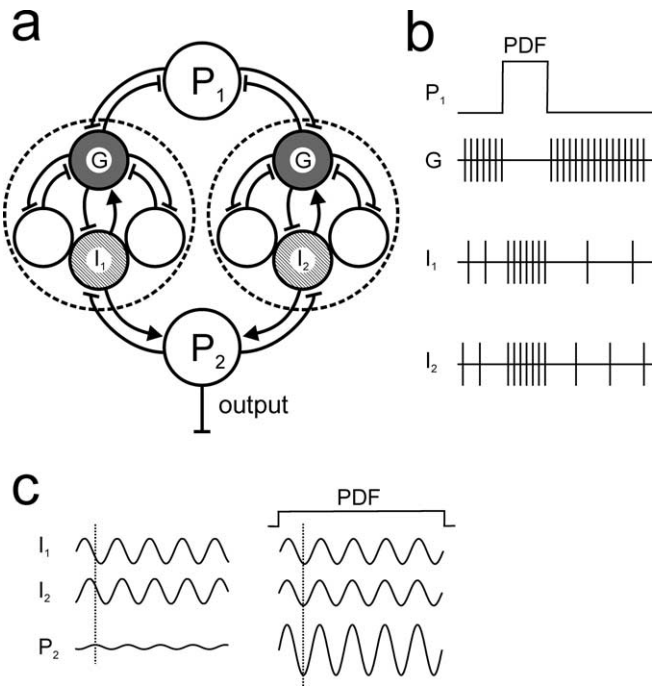

Figure 9. ***a–c***, Model of the PDF-dependent gating mechanism. ***a***, In the AMe, GABAergic interneurons (G) form assemblies of phase-locked endogenous oscillators. Within an assembly, all cells have the same phase and period, whereas between assemblies, constant phase differences are maintained via nonsynaptic, unknown mechanisms. As further illustrated with schematically drawn action potentials (***b***), PDF release from coupling elements (P_1) phase locks assemblies via inhibition of GABAergic interneurons. Thereby, postsynaptic cells ($I_{1,2}$) are disinhibited. The disinhibition and phase locking of different assemblies allows activation of their jointly controlled postsynaptic cells (P_2) via resonance. ***c***, When membrane potential oscillations of the presynaptic cells ($I_{1,2}$) become phase locked with the potential oscillations of the postsynaptic cell (P_2), the postsynaptic cell resonates; the superposition of endogenous rhythmic depolarizations with input-dependent depolarizations causes P_2 to reach threshold and fire action potentials. Therefore, we hypothesize that neuropeptide-dependent phase locking of neuronal oscillators activates the output of the pacemaker centers to locomotor control centers via resonance.

postsynaptic cell expresses membrane potential oscillations in synchrony with presynaptic oscillating neurotransmitter release, and thus neurotransmitter-induced depolarizations add up with subthreshold membrane depolarizations, causing the otherwise inactive postsynaptic cell to fire (Izhikevich et al., 2003). Thus, our results suggest that the circadian clock is a network of interconnected oscillators, which uses the control of phase relationships between ultradian membrane potential oscillations to gate various outputs via neuropeptides (Fig. 9).

References

Bloch G, Solomon SM, Robinson GE, Fahrbach SE (2003) Patterns of PERIOD and pigment-dispersing hormone immunoreactivity in the brain of the Eur honeybee *Apis mellifera*: age- and time-related plasticity. J Comp Neurol 464:269–284.

Block G, Geusz M, Khalsa S, Michel S, Whitmore D (1995) Cellular analysis of a molluscan retinal biological clock. Ciba Found Symp 183:51–60.

Cahill GM, Menaker M (1989) Responses of the suprachiasmatic nucleus to retinohypothalamic tract volleys in a slice preparation of the mouse hypothalamus. Brain Res 479:65–75.

Cheng MY, Bullock CM, Li C, Lee AG, Bermak JC, Belluzzi J, Weaver DR, Leslie FM, Zhou QY (2002) Prokineticin 2 transmits the behavioural circadian rhythm of the suprachiasmatic nucleus. Nature 417:405–410.

Christensen TA, Pawlowski VM, Lei H, Hildebrand JG (2000) Multi-unit recordings reveal context-dependent modulation of synchrony in odor-specific neural ensembles. Nat Neurosci 3:927–931.

De Jeu M, Pennartz C (2002) Circadian modulation of GABA function in the rat suprachiasmatic nucleus: excitatory effects during the night phase. J Neurophysiol 87:834–844.

Fischer J (2002) Immunocytochemie des Uhrproteins PERIOD bei der Schabe *Leucophaea maderae*. Diplome thesis, Philipps University of Marburg.

Gross GA, Hendriks J (1979) Regularly firing neurones in the rat suprachiasmatic nucleus. Experientia 35:1597–1598.

Groves PM, Wilson CJ, MacGregor RJ (1978) Neuronal interactions in the substantia nigra revealed by statistical analysis of spike trains. In: Interaction between putative neurotransmitters (Garattini S, Pujol F, Samanin R, eds), pp 191–215. New York: Raven.

Helfrich-Förster C (1995) The period clock gene is expressed in central nervous system neurons which also produce a neuropeptide that reveals the projections of circadian pacemaker cells within the brain of *Drosophila melanogaster*. Proc Natl Acad Sci USA 92:612–616.

Helfrich-Förster C (2004) The circadian clock in the brain: a structural and functional comparison between mammals and insects. J Comp Physiol [A] 190:601–613.

Helfrich-Förster C, Homberg U (1993) Pigment-dispersing hormone-immunoreactive neurons in the nervous system of wild-type *Drosophila melanogaster* and of several mutants with altered circadian rhythmicity. J Comp Neurol 337:177–190.

Helfrich-Förster C, Stengl M, Homberg U (1998) Organization of the circadian system in insects. Chronobiol Int 15:567–594.

Helfrich-Förster C, Täuber M, Park JH, Mühlig-Versen M, Schneuwly S, Hofbauer A (2000) Ectopic expression of the neuropeptide pigment-dispersing factor alters behavioral rhythms in *Drosophila melanogaster*. J Neurosci 20:3339–3353.

Homberg U, Würden S, Dircksen H, Rao KR (1991) Comparative anatomy of pigment-dispersing hormone-immunoreactive neurons in the brain of orthopteroid insects. Cell Tissue Res 266:343–357.

Homberg U, Reischig T, Stengl M (2003) Neural organization of the circadian system of the cockroach *Leucophaea maderae*. Chronobiol Int 20:577–591.

Honma S, Honma K (2003) The biological clock: Ca^{2+} links the pendulum to the hands. Trends Neurosci 26:650–653.

Izhikevich E, Desai NS, Walcott EC, Hoppensteadt FC (2003) Bursts as a unit of neural information: selective communication via resonance. Trends Neurosci 26:161–167.

Jacklet JW (1988) Circadian pacemaker neurons: membranes and molecules. J Physiol (Paris) 83:164–171.

Jiang Z, Yang YQ, Allen CN (1997) Tracer and electrical coupling of rat suprachiasmatic nucleus neurons. Neuroscience 77:1059–1066.

Kaneko M, Hall JC (2000) Neuroanatomy of cells expressing clock genes in *Drosophila*: transgenic manipulations of the *period* and *timeless* genes to mark the perikarya of circadian pacemaker neurons and their projections. J Comp Neurol 422:66–94.

Klevecz RR, Kauffman SA, Shymko RM (1984) Cellular clocks and oscillators. Int Rev Cytol 184:97–128.

Klevecz RR, Pilliod J, Bolen J (1991) Autogenous formation of spiral waves by coupled chaotic attractors. Chronobiol Int 8:6–13.

Kunz H, Achermann P (2003) Simulation of circadian rhythm generation in the suprachiasmatic nucleus with locally coupled self-sustained oscillators. J Theor Biol 224:63–78.

Laurent G (2002) Olfactory network dynamics and the coding of multidimensional signals. Nat Rev Neurosci 3:884–895.

Lee D, Sue H, O'Dowd DK (2003) GABA receptors containing Rdl subunits mediate fast inhibitory synaptic transmission in *Drosophila* neurons. J Neurosci 23:4625–4634.

Lin Y, Stormo D, Taghert PH (2004) The neuropeptide pigment-dispersing factor coordinates pacemaker interactions in the *Drosophila* circadian system. J Neurosci 24:7951–7957.

Liu C, Reppert SM (2000) GABA synchronizes clock cells within the suprachiasmatic circadian clock. Neuron 25:123–128.

Loesel R, Homberg U (1998) Sustained oscillations in an insect visual system. Naturwissenschaften 85:238–240.

Loesel R, Homberg U (2001) Anatomy and physiology of neurons with processes in the accessory medulla of the cockroach *Leucophaea maderae*. J Comp Neurol 439:193–207.

Michel S, Colwell CS (2001) Cellular communication and coupling within the suprachiasmatic nucleus. Chronobiol Int 18:579–600.

Moore R, Speth JC (1993) GABA is the principle neurotransmitter of the circadian system. Neurosci Lett 150:112–116.

Nishiitsutsuji-Uwo J, Pittendrigh CS (1968) Central nervous system control of circadian rhythmicity in the cockroach. II. The optic lobes, locus of the driving oscillator? Z Vgl Physiol 58:14–46.

Nitabach MN, Blau J, Holmes TC (2002) Electrical silencing of *Drosophila* pacemaker neurons stops the free-running circadian clock. Cell 109:485–495.

Page TL (1982) Transplantation of the cockroach circadian pacemaker. Science 216:73–75.

Peng Y, Stoleru D, Levine JD, Hall JC, Rosbash M (2003) *Drosophila* free-running rhythms require intercellular communication. PLoS Biol 1:E13.

Pennartz CM, De Jeu MT, Geurtsen AM, Sluiter AA, Hermes ML (1998) Electrophysiological and morphological heterogeneity of neurons in slices of rat suprachiasmatic nucleus. J Physiol (Lond) 506:775–793.

Petri B, Stengl M (1997) Pigment-dispersing hormone shifts the phase of the circadian pacemaker of the cockroach *Leucophaea maderae*. J Neurosci 17:4087–4093.

Petri B, Stengl M, Würden S, Homberg U (1995) Immunocytochemical characterization of the accessory medulla in the cockroach *Leucophaea maderae*. Cell Tissue Res 282:3–19.

Petri B, Homberg U, Loesel R, Stengl M (2002) Evidence for a role of GABA and Mas-allatotropin in photic entrainment of the circadian clock of the cockroach *Leucophaea maderae*. J Exp Biol 205:1459–1469.

Pikovsky A, Rosenblum M, Kurths J (2001) Synchronization. A universal concept in nonlinear sciences. In: Cambridge nonlinear science, series 12 (Chirikov B, Cvitanovic P, Moss F, Swinney H, eds), pp 27–45. Cambridge: Cambridge UP.

Reischig T, Stengl M (1996) Morphology and pigment-dispersing hormone immunocytochemistry of the accessory medulla, the presumptive circadian pacemaker of the cockroach *Leucophaea maderae*: a light and electronmicroscopic study. Cell Tissue Res 285:306–319.

Reischig T, Stengl M (2002) Optic lobe commissures in a three-dimensional brain model of the cockroach *Leucophaea maderae*: a search for the circadian coupling pathways. J Comp Neurol 443:388–400.

Reischig T, Stengl M (2003a) Ectopic transplantation of the accessory medulla restores circadian locomotor rhythms in arrhythmic cockroaches (*Leucophaea maderae*). J Exp Biol 206:1877–1886.

Reischig T, Stengl M (2003b) Ultrastructure of pigment-dispersing hormone-immunoreactive neurons in a three-dimensional model of the accessory medulla of the cockroach *Leucophaea maderae*. Cell Tissue Res 314:421–435.

Reischig T, Stengl M (2004) Pigment-dispersing hormone (PDH)-immunoreactive neurons form a direct coupling pathway between the bilaterally symmetric circadian pacemakers of the cockroach *Leucophaea maderae*. Cell Tissue Res 318:553–564.

Renn SC, Park JH, Rosbash M, Hall JC, Taghert PH (1999) A *pdf* neuropeptide gene mutation and ablation of PDF neurons each cause severe abnormalities of behavioral circadian rhythms in *Drosophila*. Cell 99:791–802.

Sato S, Chuman Y, Matsushima A, Tominaga Y, Shimohigashi Y, Shimohigashi M (2002) A circadian neuropeptide, pigment-dispersing factor-PDF, in the last-summer cicada *Meimuna opalifera*: cDNA cloning and immunocytochemistry. Zool Sci 19:821–828.

Sattelle DB, Bai D, Chen HH, Skeer JM, Buckinham SD, Rauh JJ (2003) Bicuculline-insensitive GABA-gated Cl^- channels in the larval nervous system of the moth *Manduca sexta*. Invert Neurosci 3:37–43.

Schaap J, Bos NP, de Jeu MT, Geurtsen AM, Meijer JG, Pennartz CM (1999) Neurons of the rat suprachiasmatic nucleus show a circadian rhythm in membrane properties that is lost during prolonged whole-cell recording. Brain Res 815:154–166.

Schaap J, Pennartz CM, Meijer JH (2003) Electrophysiology of the circadian pacemaker in mammals. Chronobiol Int 20:171–188.

Sehadová H, Sauman I, Sehnal F (2003) Immunocytochemical distribution of pigment-dispersing hormone in the cephalic ganglia of polyneopteran insects. Cell Tissue Res 312:113–125.

Shibata S, Oomura Y, Hattori K, Kita H (1984) Responses of suprachiasmatic nucleus neurons to optic nerve stimulation in rat hypothalamic slice preparations. Brain Res 302:83–89.

Shinohara K, Honma S, Katsuno Y, Abe H, Honma K (1995) Two distinct oscillators in the rat suprachiasmatic nucleus in vitro. Proc Natl Acad Sci USA 92:7396–7400.

Shinohara K, Hiruma H, Funabashi T, Kimura F (2000) GABAergic modulation of gap junction communication in slice cultures of the rat suprachiasmatic nucleus. Neuroscience 96:591–596.

Sokolove PG (1975) Localization of the cockroach optic lobe circadian pacemaker with microlesions. Brain Res 87:13–21.

Stengl M, Homberg U (1994) Pigment-dispersing hormone-immunoreactive neurons in the cockroach *Leucophaea maderae* share properties with circadian pacemaker neurons. J Comp Physiol [A] 175:203–213.

Strecker GJ, Wuarin JP, Dudek FE (1997) $GABA_A$-mediated local synaptic pathways connect neurons in the rat suprachiasmatic nucleus. J Neurophysiol 87:2217–2220.

Tamada Y, Tanaka M, Munekawa K, Hayashi S, Okamura H, Kubo T, Hisa Y, Ibata Y (1998) Neuron-glia interaction in the suprachiasmatic nucleus: a double labeling light and electron microscopic immunocytochemical study in the rat. Brain Res Bull 45:181–187.

Tepper JM, Martin LP, Anderson DR (1995) $GABA_A$ receptor-mediated inhibition of rat substantia nigra dopaminergic neurons by pars reticulata projection neurons. J Neurosci 15:3092–3103.

Van den Pol AN, Tsujimoto KL (1985) Neurotransmitters of the hypothalamic suprachiasmatic nucleus: immunocytochemical analysis of 25 neuronal antigens. Neuroscience 15:1049–1086.

Wagner S, Castel M, Gainer H, Yarom Y (1997) GABA in the mammalian suprachiasmatic nucleus and its role in diurnal rhythmicity. Nature 387:298–603.

Závodská R, Sauman I, Sehnal F (2003) Distribution of PER protein, pigment-dispersing hormone, prothoracicotropic hormone, and eclosion hormone in the cephalic nervous system of insects. J Biol Rhythms 18:106–122.

Gap junctions between accessory medulla neurons appear to synchronize circadian clock cells of the cockroach *Leucophaea maderae*

Nils-Lasse Schneider and Monika Stengl

Biology, Animal Physiology Philipps-University of Marburg, 35032 Marburg, Germany

J Neurophysiol
Submitted on August 8, 2005
Accepted on November 14, 2005

Abstract: The temporal organization of physiological and behavioral states is controlled by circadian clocks in apparently all eukaryotic organisms. In the cockroach *Leucophaea maderae* lesion and transplantation studies located the circadian pacemaker in the accessory medulla (AMe). The AMe is densely innervated by GABA-immunoreactive and peptidergic neurons, among them the pigment-dispersing factor-immunoreactive circadian pacemaker candidates. The large majority of cells of the cockroach AMe spike regularly and synchronously in the gamma frequency range of 25-70 Hz due to synaptic and non-synaptic coupling. While GABAergic coupling forms assemblies of phase-locked cells, in the absence of synaptic release the cells remain synchronized but fire now at a stable phase difference. To determine whether these coupling mechanisms of AMe neurons which are independent of synaptic release are based upon electrical synapses between the circadian pacemaker cells the gap junction blockers halothane, octanol and carbenoxolone were employed in presence and absence of synaptic transmission. Here, we show that different populations of AMe neurons appear to be coupled via gap junctions to maintain synchrony at a stable phase difference. This synchronization via gap junctions is a prerequisite to phase-locked assembly formation via synaptic interactions and to synchronous gamma-type action potential oscillations within the circadian clock.

Keywords: Gap junctions, synchronization, gamma range oscillations, circadian rhythms, ultradian rhythms.

Introduction

In apparently all eukaryotic and at least some procaryotic organisms the temporal organization of physiological and behavioral states is controlled by circadian clocks. In the cockroach *Leucophaea maderae* lesion and transplantation studies (Stengl and Homberg 1994; Reischig and Stengl 2003a) located the circadian pacemaker in the accessory medulla (AMe, plural: AMae) a small neuropil situated in the anterior, ventromedial edge of the medulla of the optic lobe (Homberg et al. 1991; Petri and Stengl 1995; Reischig and Stengl 1996). Similar to the mammalian suprachiasmatic nucleus (SCN) (Van den Pol and Tsujimoto 1985; Moore and Speth 1993), the AMe is densely innervated by GABA- and peptide-immunoreactive (-ir) neurons (Petri et al. 1995, 2002). Their arborizations form different AMe compartments, the noduli, the internodular and the shell region (Petri et al. 1995; Reischig and Stengl 1996, 2003b). The noduli, as well as the internodular neuropil are densely innervated by the GABA-ir distal tract and by about 25 GABA-ir neurons located in the vicinity of the AMe (Petri et al. 2002; Reischig and Stengl 2003b). While GABA-ir neurons of the distal tract appear to form the light entrainment pathway from the compound eye (Petri et al. 1995), the GABA-ir neurons in the vicinity of the AMe appear to serve as local interneurons.

Extracellular recordings of the electrical activity of excised accessory medullae (AMae) revealed that circadian pacemaker candidates of the cockroach *Leucophaea maderae* spike regularly with frequencies between 25-70 Hz, reminiscent of the gamma frequency oscillations of mammalian brain neurons. GABAergic synaptic interactions phase-lock these oscillating neurons and form different assemblies of cells that share the same period

(interspike-interval) and the same phase (timing of spikes), while cells between assemblies differ in phase (Schneider and Stengl 2005). After disruption of synaptic transmission, AMe neurons remained synchronized but obtained a stable phase difference. Therefore, additionally non synaptic interactions appear to be sufficient for phase coupling of AMe neurons (Schneider and Stengl 2005).

To examine whether gap junctions might be involved in the synchronization of AMe neurons, as in the SCN and other mammalian brain centers (Yang and Michelson 2001; Long et al. 2005; Colwell 2005) we examined the effects of gap junction blocker on electrical activity in extracellular multiunit recordings of excised AMae. The data suggest that synaptic synchronization of AMe neurons occurs through gap junction mediated coupling allowing gamma-type oscillations of the circadian pacemaker network.

Methods

All experiments were performed on AMae of adult male cockroaches. Breeding colonies of the cockroach (*Leucophaea maderae*) were kept at the University of Marburg at 30°C and 30 % humidity, in light/dark cycles of 12:12 h, with lights on from 7 a.m. to 7 p.m. Animals were provided with dried dog food, potatoes, and water ad libitum.

The experimental animals were decapitated and the head capsule was opened to excise the AMe. Details of the preparation were described previously (Schneider and Stengl 2005). The AMe can be recognized at the ventromedial edge of the medulla beneath the bifurcation of a characteristic trachea, as shown in Petri and Stengl (1997, 1999). It was excised with a glass pipette (diameter 150 µm; Flaming/Brown Micropipette Puller, model P-97; Sutter Instruments, Novato, CA). Thus, the excised AMe has a diameter and a depth of about 150 µm containing the neuropil of the AMe with about 1000 associated cells (Reischig and Stengl 2003). As immunocytochemical experiments showed all tissue explants are expected to contain the complete AMe with all associated cells and some associated medulla cells. Explants are therefore highly enriched of AMe neurons. All experiments were performed at constant light during Zeitgebertime ZT 4-9.

A total of 43 AMae (137 experiments) were employed for application of vertebrate gap junction antagonists halothane, carbenoxolone, and octanol (see below), or of the chloride channel blocker picrotoxin. In additional control recordings EtOH (1 %) or DMSO (1 %) were applied and the ionic conditions were exchanged between normal saline and extracellular solutions without Ca^{2+} or with high Mg^{2+} (see below). All chemicals used were purchased from Sigma-Aldrich (Taufkirchen, Germany).

For the extracellular recordings, the AMe was transferred to a petri dish (diameter: 4 cm). The osmolarity of the extracellular saline (156 mM NaCl, 4 mM KCl, 6 mM $CaCl_2$, 10 mM Hepes, 5 mM glucose, 0.01 g/l phenolred, pH 7.1) was adjusted with mannitol to 380 mOsm. In the Ca^{2+}-free extracellular solution $CaCl_2$ was replaced by 1 mM EGTA. In the high Mg^{2+} solution $CaCl_2$ was replaced by 10 mM $MgCl_2$. Halothane and carbenoxolone (CBX) were dissolved and diluted in saline or extracellular solution without Ca^{2+}. Octanol and picrotoxin (PTX) were dissolved in EtOH (final concentration of 0.1-1 %) and diluted in the experimental extracellular solutions. The tissue was continuously superfused with 10 ml saline per hour at room temperature. Drugs were applied to the tissue via bath application to a chamber with a volume of 5 ml and a flow rate of 30 - 40 ml/h at the following concentrations: 0.05 - 0.1 % halothane, 0.1-1mM CBX, 1-2 mM octanol, 0.5 mM PTX.

The extracellular recording technique of excised AMe and data analysis were described previously (Schneider and Stengl 2005). Glass electrodes (0.3-1.5 MΩ) connected to an extracellular amplifier (NPI, Tamm, Germany) recorded the extracellular electrical activity of the excised AMe. Multi unit action potentials (=events) were recorded as upward and/or downward deflections of the baseline. Recordings sampled different numbers of AMe neurons. Rarely, apparently single unit recordings were obtained. It cannot be expected that we sampled all AMe neurons at the same time. The output of the amplifier was high-pass filtered (3 Hz) to eliminate electrode offset and low-pass filtered (1.5 kHz) to avoid high frequency noise and aliasing. The signal was digitized (DIGIDATA 1322A; Axon Instruments, Burlingame, CA, USA) with a sampling rate of 5 kHz, and stored on hard disc for further analysis. Event detection above a given threshold was performed offline with SPIKE II software (Cambridge Electronic Design, Cambridge, England).
The mean frequency (number of events/s) was calculated and the interevent-interval distributions were generated using 1 ms bin width, and different periods with a minimum of 100 s, at different time points of the experiment, to identify oscillations and changes in the regularity of the electrical activity.

The oscillation of the firing neurons is defined by the regularity of their action potentials. This means that the time spend between two consecutive action potentials (= the interspike interval) is the period of the oscillation and the time point at which the action potential occurs is the phase of the oscillation. Therefore, two neurons are phase-locked (with zero phase difference) if they fire action potentials at exactly the same time point, with the same phase and the same period, or integer multiples of the same period (it would not change the interspike-interval if the second cell spikes only at every second action potential of the first cell). Thus, their spike amplitudes superimpose in the original recording (larger amplitudes) and a single sharp band occurs in the instantaneous frequency plot (1/interspike-interval). Instantaneous frequency (1/interevent-interval) plots were calculated over the whole time course of the experiments to visualize the

regularity of electrical activity and to analyze the synchrony and phase coupling of the recorded cells. In the instantaneous frequency plot the electrical activity of irregularly spiking neurons, or of neurons spiking with different rates or phases that are not integer multiples of each other, result in a broad cloud of instantaneous frequencies. A defined narrow band of instantaneous frequencies means that all recorded cells fire action potentials very regularly at the same phase and at the same or integer multiples of the same interevent-interval (harmonic frequencies). Parallel bands in the instantaneous frequency plot indicate that at least two cells fire with the same or integer-multiples of the same interevent-interval, but with a stable phase difference. If more than one cell fires very regularly with different non-integer multiples of interevent-intervals and with different phase, the bands cross each other (Pikovski et al. 2001). Fusion of parallel bands to one band indicates that the recorded cells now fire with the same phase (action potentials occur at the same time) and the same period (=same interevent-intervals). Autocorrelograms were generated, using a bin width of 1 ms for an interval of 1 s over 5 -30 min periods, to identify rhythmic firing patterns (Groves et al. 1978). Regular interevent-intervals cause multiple peaks in the autocorrelogram (Tepper et al. 1995). Irregularity eliminates multiple peaks.

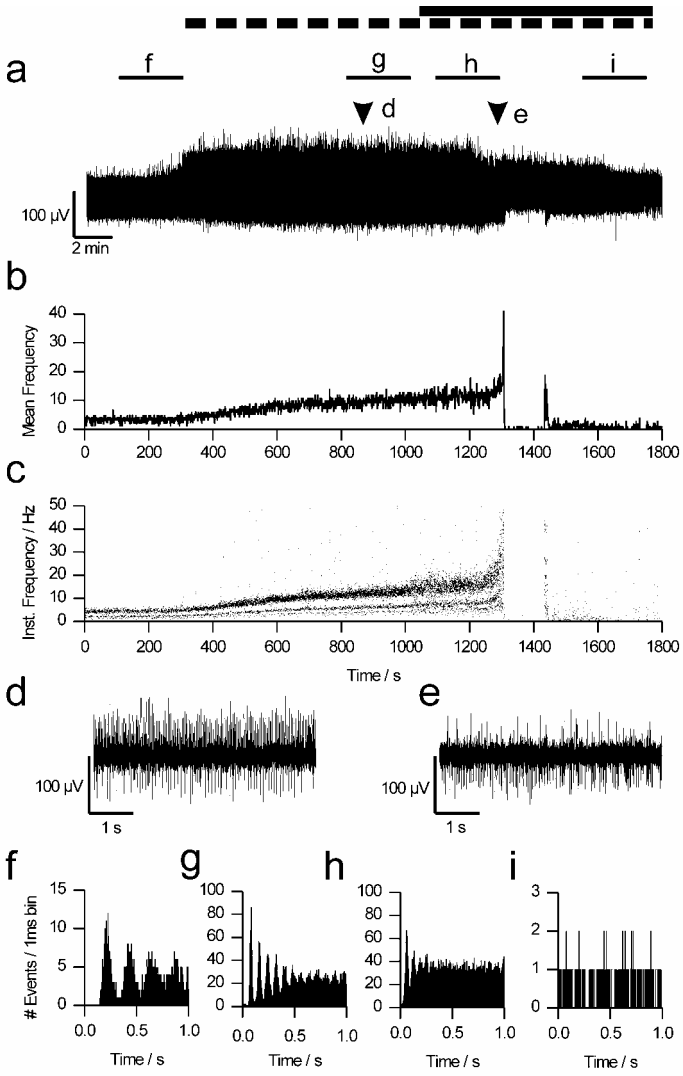

Figure 1. a-i. Gap junction inhibitors desynchronize AMe neurons in the absence of functional synaptic connections. Exchange of extracellular saline to Ca^{2+} free extracellular solution (dashed bar) disrupts synaptic release. This results in an increase of activity in the original recording (**a**) and a rise in the mean frequency (**b**). In addition the two parallel instantaneous frequency bands increase to a higher frequency level in synchrony with a newly appearing third band (**c**). After additional perfusion with 0.1 % halothane (black bar) the mean frequency transiently increases until synchronous activity abruptly ceases (**b**). The distinct bands in the instantaneous frequency plot rise, broaden, and become diffuse until sudden cease of synchronous activity (**c**). The original recordings (extended timescales at time points **d** and **e** in **a,** downward deflections of the base line were evaluated) and the autocorrelograms (**f - i**) show that previously coupled neurons loose phase-locking and fire irregularly during disruption of gap junctions. Same time axes for **a-c**. Thin bars (f, g, h, i) indicate the time window for autocorrelation analysis (**f, g, h, i**).

Results

In extracellular multi-unit recordings of the isolated AMe, the cockroach circadian pacemaker center, the gap junction antagonists halothane, carbenoxolone, and octanol were employed, to test whether they affect the synchronization of AMe neurons. We show that the gap junction antagonists desynchronize most, but not all AMe neurons in the presence and absence of synaptic release. We hypothesize that gap junctions between inhibitory interneurons are essential for phase-coupling of circadian pacemaker candidates within the AMe network.

Extracellular recordings of multiunit electrical activity (events) of the excised AMe lasted for several hours. Events were recorded as upward and downward deflections of the baseline (Fig. 1a) depending on the impedance ratio between the recorded neurons, the recording electrode and the indifferent electrode. Event amplitudes ranged from 50 to 180 µV whereas the average peak-to-peak noise amplitude was about 40 µV. As described earlier electrical activity within the excised AMe is reversibly blocked by the sodium channel blocker tetrodotoxin (Schneider and Stengl 2005). In about 76 % (of 37 preparations) the electrical activity of AMe neurons oscillated regularly (period of the oscillation = interspike-interval, phase = occurrence of spikes). Synchronous regular spiking is not recognizable in the mean event frequency (Fig. 1b), but is obvious in instantaneous frequency plots (Fig. 2c), at an extended time scale of the original recordings (Fig. 2 d), in interevent-interval distributions (Fig. 2 f-h), and autocorrelation analysis of event-times (Fig. 2i, j). These methods of analysis revealed that recorded AMe neurons were synchronized and fired with

constant interevent-intervals and at stable phase relationships. Spontaneous activity exhibited 1 to 3 distinct parallel bands in the instantaneous frequency plot (see Materials and Methods). Multiunit activity resulting in one band in the instantaneous frequency plot originates from synchronized cells firing at the same phase and the same or harmonic frequencies, while parallel bands originate from different assemblies of cells firing with the same or harmonic frequencies but with a stable phase difference between assemblies (Materials and methods).

In 71% of the recordings cells remained synchronized after disruption of synaptic interactions, while in 29 % of the preparations cells require synaptic interactions for synchronization. Thus, as suggested previously, mechanisms of phase coupling in addition to inhibitory synaptic interactions are employed to form assemblies, (Schneider and Stengl 2005). To test whether gap junction mediated coupling is responsible for retaining a constant phase relationship after disruption of synaptic release, we applied the gap junction blocker halothane in the presence of Ca^{2+} free extracellular solution (n=10 in 7 preparations) (Fig. 1a-i). Application of 0.05-0.1 % halothane caused a decrease in the amplitude of the electrical events in the original recording (Fig. 1a) and a transient increase and then, strong decrease in the mean frequency (Fig. 1b). The diffusion of distinct bands in the instantaneous frequency plot (Fig. 1c) and simultaneous changes in the mean frequency occurred within 1-3 min in 86 % of the preparations (n=8 in 6 preparations). The delay of the halothane effect was dose-dependent and took longer at lower blocker concentrations (Table 1). Details of the original recordings (Fig. 1d, e) and autocorrelation analysis after application of 0.1 % halothane revealed that synchronization of neuronal activity is lost (compare Figs. 1f-i). In 86 % of the preparations (n=7 in 6 preparations, not shown) the cells started to burst, until complete loss of synchronization occurred. In 71 % (n=5 in 5 preparations) of the preparations activity ceased completely in the presence of halothane (Fig. 1).

To determine whether coupling via chemical synapses also depends on synchronization via gap junctions (Figs. 2, 3) we employed halothane and other gap junction blockers in normal saline (n=40 in 22 preparations). Even in the presence of synaptic interactions, application of 0.1 % halothane (n=20 in 15 preparations) disrupts the synchronization of AMe neurons in 67 % of the preparations (Fig. 2; n=15 in 10 preparations). Halothane changed the amplitude of the electrical events in the original recording (Fig. 2a). It first caused an increase of the mean frequency (Fig. 2b) and a broadening of the instantaneous frequency band (Fig. 2c). The diffusion of the instantaneous frequency band was accompanied by the appearance of bursting activity in 40 % of these recordings (Figs. 2 c-e). The

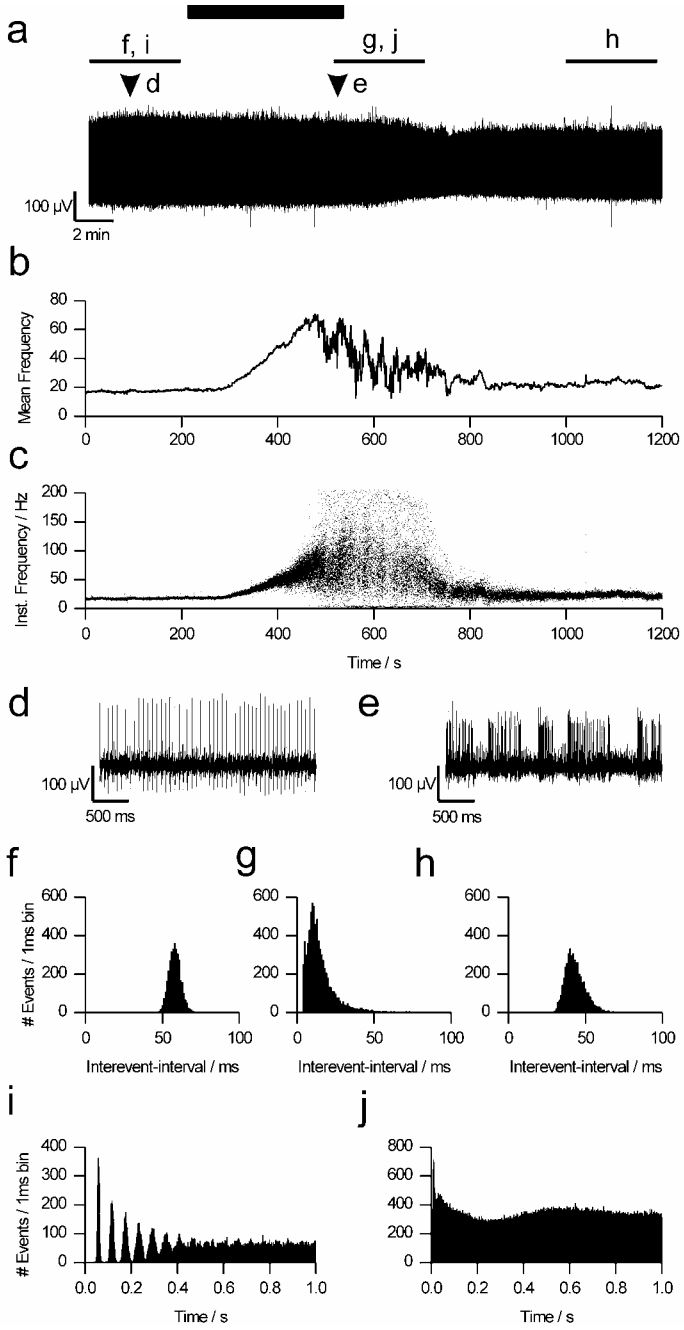

Figure 2. a-j. The gap junction antagonist halothane reversibly disrupts phase coupling of AMe neurons in the presence of synaptic interactions. During superfusion with normal saline AMe neurons fire synchronously at the same low frequency and the same phase. This is shown in the original recording (**a**), and the mean frequency (**b**). It also becomes apparent in the single band in the instantaneous frequency plot (**c**), the original trace at an extended timescale at time point **d,** the sharp peak in the interspike-interval distribution (**f**), and the multiple peaks in the autocorrelogram (**i**). During application of 0.1 % halothane (black bar in **a**) the mean frequency increases (**b**) and the previously distinct band in the instantaneous frequency plot broadens and becomes more and more irregular with superimposed variable bursts. The expanded time scale (**e**) and the autocorrelogram (**j**) show that AMe neurons loose stable phase coupling.

broadening and shift in the interevent-interval distribution (Figs. 2 f-h), and loss of multiple peaks in the autocorrelogram (compare Figs. 2 i, j) further show loss of coordinated electrical activity. Finally, in almost all preparations, activity ceased completely after application of halothane (not shown). After wash out of the gap junction blocker AMe neurons returned to regular firing with zero phase difference in 70 % of the preparations (n=7 in 7 preparations) as can be seen in the narrowing of the instantaneous frequency band (Fig. 2 c) and the defined peak in the interevent-interval histogram (Fig. 2 h).

To test, whether also other gap junction inhibitors mimic the effects of halothane we employed the gap junction antagonists octanol (n=4, in 3 preparations) and carbenoxolone (CBX, n=14 in 9 preparations) in normal saline (Fig. 3). Also, these gap junction blockers usually resulted in a dose dependent, strong, and sustained decline of synchronous electrical activity in normal extracellular saline (Figs. 3 a-d; Table 1). Mostly (but not in all applications) irreversible loss of synchronous activity were caused by application of 0.1-1 mM CBX with dose dependent time delays (Figs. 3 b, c) (n=11 in 8 preparations). The sustained inhibition of electrical activity caused by CBX was removed and the cells became irregularly active by disrupting synaptic transmission via superfusion with Ca^{2+} free extracellular solution (Fig. 3 d) or via application of the chloride channel blocker picrotoxin (PTX) (not shown). Also halothane and octanol-dependent loss of activity could be reversed to irregular activity by Ca^{2+}-free solutions (not shown). Since octanol and PTX were dissolved in EtOH (final concentration: 0.1-1 %) respective control experiments were performed. Application of saline with 1 % EtOH showed no effects on electrical activity of AMe neurons.

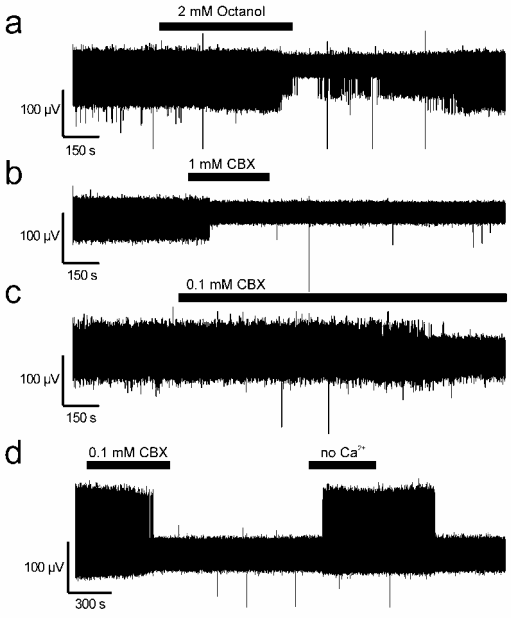

Figure 3. a-d. Gap junction antagonists octanol and carbenoxolone (CBX) inhibit AMe neurons in the presence of synaptic interactions. **a**, application of 2 mM octanol (black bar) reversibly inhibits AMe neurons in normal extracellular saline. **b, c**, application of CBX causes mostly irreversible inhibitions with dose dependent time delays. **d,** Neuronal activity inhibited by 0.1 mM CBX resumes in saline without Ca^{2+} which disrupts synaptic interactions.

Previous studies have shown that GABAergic interneurons coordinate the synchronized, regular spiking of AMe neurons (Petri et al. 2002; Schneider and Stengl 2005). To obtain information whether cells which synchronize AMe neurons independent of GABA are also coupled via gap junctions, we employed halothane in the presence of PTX (Lee et al. 2003; Sattelle et al. 2003). PTX was shown previously to oppose GABA-dependent inhibitions and, thus, can be used as $GABA_A$ receptor antagonist in the cockroach (Schneider and Stengl 2005). In the presence of 0.5 mM PTX cells which fired at a low frequency (Fig. 4 a, b, d, f, j), showed a reversible increase of mean electrical activity after application of 0.1 % halothane (Fig. 4 a, b, e, g, k). In addition, in the presence of PTX halothane resulted in a coordinated broadening of the previously narrow band of instantaneous frequency (Fig. 4 b), and reversibly changed the firing mode into regular bursting in 75 % of the preparations (n=8, in 3 of 4 preparations) (Fig. 4 compare d, e). Other AMe neurons retained synchrony in the presence of PTX and were not affected by application of halothane (Figs. 4 c, h, i, l, m) (n=3, in 2 preparations).

Discussion

Multiunit recordings from excised AMae, the circadian pacemaker centers of the cockroach *Leucophaea maderae*, were utilized to investigate the effects of gap junction blockers on synchronization of neuronal spike discharges of circadian pacemaker cells. Evidence is provided that different populations of AMe neurons are coupled via gap junctions maintaining synchronous activity at a stable phase difference. Synchronization via gap junctions also appears to be a prerequisite to synchronization via synaptic interactions. These different types of synchronization mechanisms cause regular action potential oscillations with precision on the millisecond scale, firing at frequencies of 25-80 Hz, reminiscent of gamma-frequency oscillations in networks of the mammalian brain.

Electrical synapses appear to be present in the circadian pacemaker center

Our experiments suggest that AMe neurons use gap junction-mediated coupling as additional mechanisms of synchronization. Because different vertebrate gap junction blockers caused the same effects, dose-dependently and reversibly, it is very likely that these gap junction blockers specifically block cockroach gap junctions. Additional evidence for the presence of gap junctions between cockroach AMe neurons comes from intracellular recordings in the AMe of *L. maderae* (Loesel and Homberg 2001). Because in the

vast majority of these intracellular recordings multiple stainings were obtained it is likely that the injected dye was spreading through gap junctions. Further evidence for the specificity of the vertebrate gap junction blockers in the invertebrates comes from a comparison of their effects between invertebrate and vertebrate preparations. In the SCN several experimental approaches demonstrated the presence of electrical synapses. Two-cell patch clamp recordings showed that mammalian SCN neurons are electrically coupled via gap junctions and promote synchronization of electrical activity on the millisecond scale, similar to cockroach AMe neurons (Long et al. 2005). Furthermore, dye coupling experiments, immunocytochemical studies and mutant analysis showed that gap junction molecules are present in the SCN and are necessary for synchronization of circadian pacemaker candidates (Jiang et al. 1997; Colwell 2000; Shinohara et al. 2000; Schaap et al. 2003; Long et al. 2005).

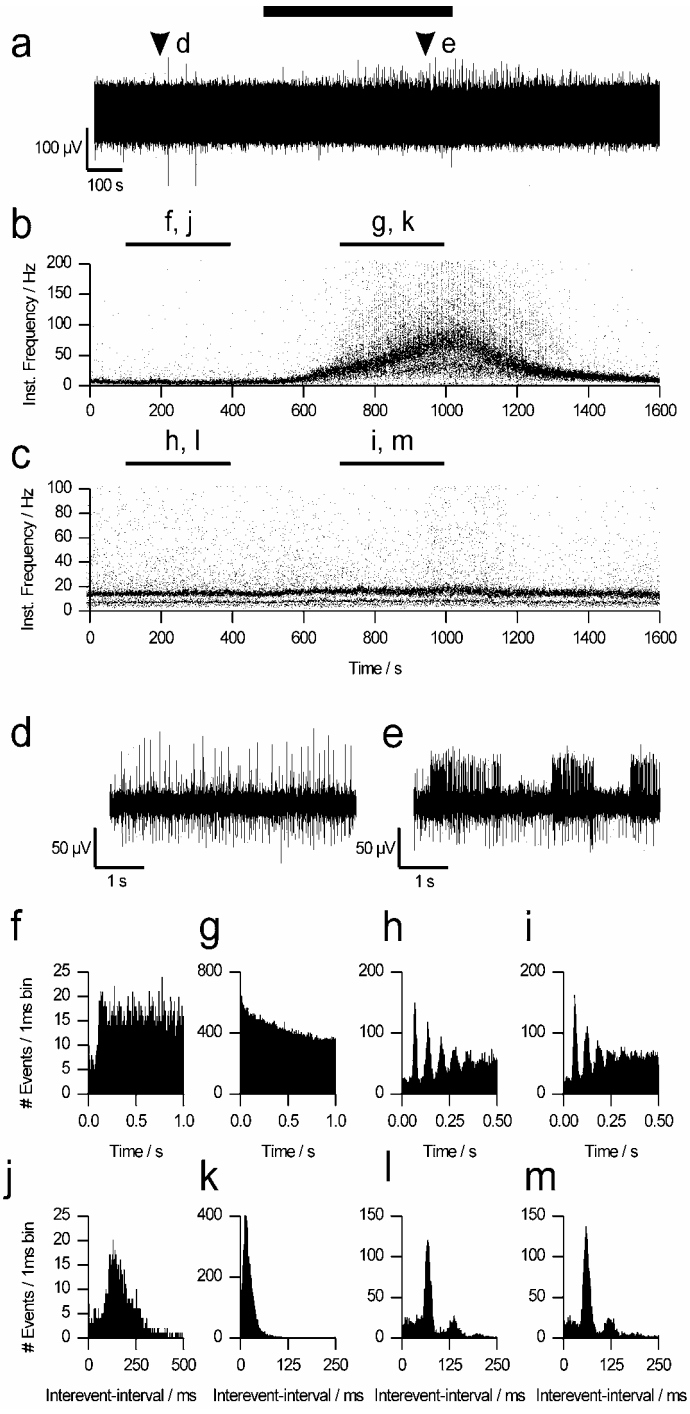

Figure 4. a-m. In the presence of the chloride channel blocker picrotoxin (PTX) the gap junction antagonist halothane increases and desynchronizes the electrical activity of a subgroup of recorded AMe neurons, while other neurons are unaffected. Upward deflections from the baseline are evaluated in **b**, **f**, **g**, **j**, **k**. Downward deflections are evaluated in **c**, **h**, **i**, **l**, **m**. During the constant presence of 0.5 mM PTX synchronized assemblies of cells could be recorded (**a**) which formed the sharp bands in the instantaneous frequency plots (**b, c**). The same time axis is used in **a-c**. When 0.1 % halothane was added (black bar in **a**) the assembly in **b** increased its instantaneous frequency and started to burst, while the synchronized assemblies in **c** remained phase locked to a stable phase difference. Original trace at an extended timescale at time points **d** and **e** in **a** further illustrates that bursting develops after addition of halothane. Thin bars in **b** and **c** indicate the time windows for autocorrelation analysis and interevent-interval distribution (**f–m**).

Which cells are connected via gap junctions in circadian pacemaker centers?

Neurons of the cockroach circadian pacemaker center exhibit regular spike discharges with precision on the millisecond scale. They form assemblies of phase-locked, synchronously firing AMe cells via GABA-release at synapses and via unknown non-(chemically) synaptic mechanisms (Schneider and Stengl 2005). Since in 29 % of the preparations AMe neurons desynchronized after disruption of synaptic transmission at least some assemblies appear to be formed solely by chemical synapses. The majority of the AMe cells, however, rely on additional mechanisms of synchronization. Gap junction blockers caused persistent inhibitions in normal saline, in the presence of functional chemical synapses. These inhibitions could be released via interruption of synaptic transmission and via block of $GABA_A$ receptors in the presence of gap junction blockers. Therefore, the inhibitions were most likely due to blocker-dependent desynchronization of GABA-ergic interneurons. Thus, apparently at least subpopulations of GABAergic interneurons are synchronized via gap junctions and the electrical synapses are a prerequisite to GABA-dependent assembly formation. But also in the presence of PTX, when already all $GABA_A$-receptor dependent synchronization was lost remaining synchronization mechanisms were interrupted and inhibitory interactions were released via gap junction blockers. Therefore, next to GABAergic interneurons there are additional inhibitory interneurons which appear to be coupled via gap

junctions. Very rarely $GABA_B$-dependent inhibitions were observed in the AMe, but more often peptide-dependent inhibitions were obtained. Thus, it is likely that subpopulations of inhibitory peptidergic neurons of the AMe such as pigment-dispersing factor containing neurons might be coupled via electrical synapses (Schneider and Stengl 2005).

Table 1. Effects of gap junction antagonists show dose dependent time delays/min

	conc.	delay	
Halothane	0.1 %	2.1 ± 1.3	n = 15
	0.05 %	4.0 ± 0.5	n = 5
Carbenoxolone	1 mM	2.9 ± 0.2	n = 2
	0.1 mM	11.9 ± 1.9	n = 6

The mammalian circadian pacemaker cells also remained weakly coupled after removal of extracellular Ca^{2+}, but lost coupling in the presence of gap junction blockers (Bouskila and Dudek 1993; Jiang et al. 1997; Colwell 2000; Shinohara et al. 2000; Long et al. 2005). As in the cockroach, gap junctions in the SCN couple circadian pacemaker candidates to synchronized phase-locked assemblies. The assemblies of different regions of the SCN are then coupled via synaptic interactions such as via GABAergic and peptidergic neurons (Itri and Colwell 2003; Colwell 2005; Albus et al. 2005). Therefore, it is assumed in the circadian pacemaker centers of mammals and, shown here in the cockroach alike that electrical synapses are a prerequisite for synchronous, regular action potential oscillations with precision on the millisecond scale. But the functional significance of gap-junction dependent electrical synchrony in the ultradian range is largely unknown in the circadian pacemaker centers.

Functions of gap-junction-dependent synchronized action potential oscillations in circadian pacemaker centers

More about the function of electrical synapses in neuronal networks is known in other regions of the vertebrate brain. In the locus ceruleus electrotonic coupling synchronizes spontaneous firing of neurons dependent on their firing rates (Alvarez et al. 2002). Computational modeling demonstrated that coupling of non-oscillating cells via gap junctions can generate synchronized membrane potential oscillations (Loewenstein et al. 2001). Thus, electrical synapses are widely used in the mammalian brain to generate synchronized neuronal activity, also in the range of 30-80 Hz (Jedlicka and Backus 2005). This so called gamma rhythm was proposed to be essential for induction of spike timing-dependent synaptic plasticity, for memory processes, and for "binding" of sensory object features into coherent conscious percepts (Engel and Singer 2001; Jedlinca and Draguhn 2005).

It is largely unresolved why it is important for circadian pacemaker neurons to express synchronized action potential oscillations with high precision on the millisecond scale in the range of 25-80 Hz, reminiscent of the mammalian gamma rhythms. For the cockroach circadian clock Schneider and Stengl (2005) suggested that neuropeptide-dependent phase control of these regular oscillating action potential rhythms are used for gating different circadian outputs such as circadian locomotor activity rhythms via resonance. It is suggested that the circadian clocks main task is to synchronize, to determine, and maintain the phase relationships of the different physiological processes in the body within the 24 hour cycle of light and dark. Thus, the clock is active throughout the day to determine at what sequence and with what phase-relationship all the different physiological processes in the body take place, in synchrony with external rhythms. Since information processing in the brain depends on mechanisms of temporal encoding with precision on the millisecond scale, also the circadian clock as part of the brain is based upon these principles. Neuropeptide-dependent gating might also be employed in the mammalian circadian clock, because the neuropeptide vasoactive intestinal polypeptide (VIP) mediates rhythmicity and synchrony in the SCN (Aton et al. 2005) and VIP-receptor-knockouts show impaired locomotor activity rhythms (Harmar et al. 2002). Furthermore, in connexin 36-knockout mice without gap junctions circadian activity rhythms dampened and delayed in constant darkness (Long et al. 2005). Not only on the network level, but also for single circadian pacemaker cells electrical activity on the millisecond scale and circadian rhythms appear to be intimately interconnected, because electrically silencing stops clock gene rhythms (Nitabach et al. 2002). Further experiments will test whether gap-junction mediated synchronous oscillations of AMe neurons is a necessary prerequisite to circadian clock gene rhythms and to circadian locomotor activity outputs in the cockroach.

Acknowledgements

We thank Dr. Uwe Homberg (University of Marburg) and unknown referees for improvement of the manuscript. The work was supported by DFG grant STE531/15-1.

References

Albus H, Vansteensel MJ, Michel S, Block GD, and Meijer H. A GABAergic mechanism is necessary for coupling dissociable ventral and dorsal regional oscillators within the circadian clock. *Current Biol* 15: 886-893, 2005.

Alvarez VA, Chow CC, Van Bockstaele EJ, and Williams JT. Frequency-dependent synchrony in locus ceruleus: role of electrotonic coupling. *Proc Natl Acad Sci USA* 99: 4032-4036, 2002.

Aton SJ, Colwell CS, Harmar AJ, Waschek J, and Herzog ED. Vasoactive intestinal polypeptide mediates circadian rhythmicity and synchrony in

mammalian clock neurons. *Nat Neurosci* 8: 476-483, 2005.

Bouskila Y and Dudek FE. Neuronal synchronization without calcium-dependent synaptic transmission in the hypothalamus. *Proc Natl Acad Sci USA* 84: 1694-1698, 1993.

Colwell CS. Rhythmic coupling among cells in the suprachiasmatic nucleus. *J Neurobiol* 43: 379-388, 2000.

Colwell CS. Bridging the gap: coupling single cell oscillators in the suprachiasmatic nucleus. *Nat Neurosci* 8: 10-12, 2005.

Engel AK and Singer W. Temporal binding and the neural correlates of sensory awareness. *Trends Cogn Sci* 5: 16-25, **2001**

Groves PM, Wilson CJ, and MacGregor RJ. Neuronal interactions in the substantia nigra revealed by statistical analysis of spike trains. In: *Interaction between putative neurotransmitters*, edited by Garattini S, Pujol F, Samanin R. New York: Raven; 1978, pp. 191-215.

Harmar A, Marston H, Shen S, Spratt C, West K, Sheward W, Morrison C, Dorin J, Piggins H, and Reubi J. The VPAC2 Receptor Is Essential for Circadian Function in the Mouse Suprachiasmatic Nuclei. *Cell* 109: 497-508, 2002.

Helfrich-Förster C. The period clock gene is expressed in central nervous system neurons which also produce a neuropeptide that reveals the projections of circadian pacemaker cells within the brain of *Drosophila melanogaster*. *Proc Natl Acad Sci USA* 92: 612-616, 1995.

Homberg U, Würden S, Dircksen H, and Rao KR. Comparative anatomy of pigment-dispersing hormone-immunoreactive neurons in the brain of orthopteroid insects. *Cell Tissue Res* 266: 343-357, 1991.

Itri J and Colwell CS. Regulation of inhibitory synaptic transmission by vasoactive intestinal peptide (VIP) in the mouse suprachiasmatic nucleus. *J Neurophysiol* 90: 1589-1597, 2003.

Jedlicka P and Backus KH. Inhibitory transmission, activity-dependent ionic changes and neuronal network oscillations. *Physiol Res*, 2005.

Jiang Z, Yang YQ, and Allen CN. Tracer and electrical coupling of rat suprachiasmatic nucleus neurons. *Neuroscience* 77: 1059-1066, 1997.

Loesel R and Homberg U. Anatomy and physiology of neurons with processes in the accessory medulla of the cockroach *Leucophaea maderae*. *J Comp Neurol* 439: 193-207, 2001.

Loewenstein Y, Yarmon Y, and Sompolinski H. The generation of oscillations in networks of electrically coupled cells. J *Neurobiol* 98: 8095-8100, 2001.

Long MA, Michael JJ, Conners BW, and Burwell RD. Electrical synapses coordinate activity in the suprachiasmatic nucleus. *Nature Neurosci* 8: 61-66, 2005.

Moore R and Speth JC. GABA is the principle neurotransmitter of the circadian system. *Neurosci Lett* 150: 112-116, 1993.

Nitabach MN, Blau J, and Holmes TC. Electrical silencing of *Drosophila* pacemaker neurons stops the free-running circadian clock. *Cell* 109: 485-495, 2002.

Petri B, Stengl M, Würden S, and Homberg U. Immunocytochemical characterization of the accessory medulla in the cockroach *Leucophaea maderae*. *Cell Tissue Res* 282: 3-19, 1995.

Petri B and Stengl M. Presumptive insect circadian pacemakers in vitro: immunocytochemical characterization of cultured pigment-dispersing hormone-immunoreactive neurons of *Leucophaea maderae*. *Cell Tissue Res* 296: 635-431, 1999.

Petri B, Homberg U, Loesel R, and Stengl M. Evidence for a role of GABA and Mas-allatotropin in photic entrainment of the circadian clock of the cockroach *Leucophaea maderae. J Exp Biol* 205: 1459-1469, 2002.

Pikovsky A, Rosenblum M, and Kurths J. Synchronization. A universal concept in nonlinear sciences. Chirikov B., Cvitanovic P., Moss F., Swinney H. (eds.) Cambridge Nonlinear Science Series 12, Cambridge University Press, 2001.

Reischig T and Stengl M. Morphology and pigment-dispersing hormone immunocytochemistry of the accessory medulla, the presumptive circadian pacemaker of the cockroach *Leucophaea maderae*: a light and electronmicroscopic study. *Cell Tissue Res* 285: 306-319, 1996.

Reischig T and Stengl M. Ectopic transplantation of the accessory medulla restores circadian locomotor rhythms in arrhythmic cockroaches (*Leucophaea maderae*). *J Exp Biol* 206:1877-1886, 2003a.

Reischig T and Stengl M. Ultrastructure of pigment-dispersing hormone-immunoreactive neurons in a three-dimensional model of the accessory medulla of the cockroach *Leucophaea maderae*. *Cell Tissue Res* 314:421-435, 2003b.

Schaap J, Pennartz CMl, and Meijer JH. Electrophysiology of the circadian pacemaker in mammals. *Chronobiol Int* 20:171-188, 2003.

Schneider NL and Stengl, M. Pigment-dispersing factor and GABA synchronize cells of the isolated circadian clock of the cockroach *Leucophaea maderae*. *J Neurosci* 25:5138-5147, 2005.

Shinohara K, Hiruma H, Funabashi T, and Kimura F. GABAergic modulation of gap junction communication in slice cultures of the rat suprachiasmatic nucleus. *Neuroscience* 96:591-596, 2000.

Stengl M and Homberg U. Pigment-dispersing hormone-immunoreactive neurons in the cockroach

Leucophaea maderae share properties with circadian pacemaker neurons. *J Comp Physiol* A 175:203-213, 1994.

Tepper JM, Martin LP, and Anderson DR. $GABA_A$ receptor-mediated inhibition of rat substantia nigra dopaminergic neurons by pars reticulata projection neurons. *J Neurosci* 15:3092-3103, 1995.

Van den Pol AN and Tsujimoto KL. Neurotransmitters of the hypothalamic suprachiasmatic nucleus: immunocytochemical analysis of 25 neuronal antigens. *Neuroscience* 15:1049-1086, 1985.

Yang Q and Michelson HB. Gap junctions synchronize the firing of inhibitory interneurons in guinea pig hippocampus. *Brain Research* 907:139-143, 2001.

Extracellular long-term recordings of the isolated circadian pacemaker center of the cockroach *Leucophaea maderae* reveal circadian as well as ultradian rhythms

Nils-Lasse Schneider and Monika Stengl

Biology, Animal Physiology, Philipps-University of Marburg, 35032 Marburg, Germany

J Neurophysiol
Submitted on November 23, 2005

Abstract: In the cockroach *Leucophaea maderae* transplantation and lesion studies located the circadian pacemaker center which controls locomotor activity rhythms to the accessory medulla (AMe), ventromedially to the medulla of the brain's optic lobes. The AMe is densely innervated via GABA- and peptide-immunoreactive neurons which express ultradian action potential oscillations in the gamma frequency range and form phase locked assemblies of synchronously spiking cells. So far, it remained unknown whether the electrical activity of the isolated insect circadian clock also expresses circadian rhythms.

In extracellular glass electrode recordings of the isolated AMe we examined the distribution of activity peaks independently of the absolute action potential frequency. We show that electrical activity peaks are predominantly distributed to the mid-subjective night, with a minimum at the middle of the day. Additionally, the analysis of electrical activity peak distributions revealed ultradian periods, which are multiples of a fundamental 2 hours period. We hypothesize that changes in electrical activity are correlated with peptide release and that circadian rhythms originate from coupled ultradian oscillations.

Keywords: Long-term recordings, circadian rhythms, ultradian rhythms, accessory medulla

Introduction

Circadian clocks control the temporal order of physiological and behavioral states in organisms on earth. They synchronize these internal rhythms with the environmental 24 hour cycle of light and dark. Lesion and transplantation studies located the circadian clock which controls locomotor activity rhythms of the cockroach *Leucophaea maderae* to the accessory medulla (AMe; plural: AMae) (Stengl and Homberg 1994; Reischig and Stengl 2004). The AMe is a small neuropil in the optic lobes at the anterior, ventromedial border of the medulla and is densely innervated by a manifold of peptide-ir and GABA-ir neurons (Homberg et. al. 1991; Petri et al. 1995, Petri et al. 2002; Reischig and Stengl 1996). Among the peptidergic cells of the AMe are the pigment-dispersing-factor (PDF)-immunoreactive (ir) neurons which are proposed to be circadian pacemaker cells in the cockroach, as well as in the fruitfly (Homberg et al. 1991, 2003; Helfrich-Förster and Homberg 1993; Stengl and Homberg 1994; Helfrich-Förster 1995; Reischig and Stengl 1996, 2004; Sato et al. 2002; Bloch et al. 2003; Sehadová et al. 2003; Závodská et al. 2003). Different AMe compartments are formed by arborizations of peptidergic neurons: the noduli, the internodular, and the shell region (Petri et al. 1995; Reischig and Stengl 1996, 2003b). The noduli and the internodular neuropil are densely innervated by the GABA-ir distal tract which appears to bring light entrainment from the compound eye into the clock. About 25 GABA-ir neurons next to the AMe extensively innervate the AMe neuropil. At least some of them appear to serve as local interneurons of the AMe which form different phase-locked neuronal assemblies.

Extracellular multiunit recordings of electrical activity of the excised AMe revealed that AMe neurons generate ultradian oscillations in their action potential responses on the ms time scale (Schneider and Stengl 2005a). The AMe neurons fire synchronously and very regularly in the gamma frequency range at 30-80 Hz due to non-neuronal as

well as neuronal coupling interactions. They are grouped into phase-locked assemblies gap junction- and GABA-dependently (Schneider and Stengl 2005a, b). Release of the peptide PDF synchronized neurons from previously different assemblies. We hypothesized that PDF release formed a new assembly of synchronously firing cells to gate locomotor outputs of the clock via disinhibitions (Schneider and Stengl 2005a). These peptide-dependent changes in synchrony were accompanied by changes in mean frequency of extracellular recorded multiunit activity. Possibly, the observed PDF-dependent disinhibitions of AMe neurons is a general scheme of peptide action in the AMe. Thus, we searched for peaks in event frequencies as a possible indicator of peptide-dependent changes in synchronization of AMe neurons throughout the day.

The data show that AMe neurons periodically increase their mean event frequency during 24 hours of constant darkness. Most changes in the mean frequency occur during the middle of the subjective night, the least occur at the middle of the day. Interestingly, next to this period in the circadian range also ultradian periods that are integer multiples of about 2 hours are predominant in the changes of electrical activity of AMe neurons.

Methods

All experiments were performed on AMae of adult male cockroaches at constant darkness. Two breeding colonies at inverse light dark cycles (12 hours apart) of the cockroach (*Leucophaea maderae*) were kept at the University of Marburg at 30°C and 30 % humidity, in light/dark cycles of 12:12 h, with lights on from 7 a.m. to 7 p.m. and 7 p.m. to 7 a.m. Animals were provided with dried dog food, potatoes, and water ad libitum.

About equal numbers of experimental animals were taken from both inverse colonies. They were decapitated and the head capsule was opened to excise the AMae at normal day light. Details of the preparation were described previously (Schneider and Stengl 2005a). The AMe can be recognized at the ventromedial edge of the medulla beneath the bifurcation of a characteristic trachea (Petri and Stengl 1997, 1999). It was excised with a glass pipette (diameter 150 µm; Flaming/Brown Micropipette Puller, model P-97; Sutter Instruments, Novato, CA). Thus, the excised AMe has a diameter and a depth of about 150 µm containing the neuropil of the AMe with about 1000 associated cells (Reischig and Stengl 2003b). All experiments were performed at constant darkness (DD).

For the extracellular recordings, the AMe was transferred to a petri dish (diameter: 4 cm). The tissue was continuously superfused with 10 ml saline (Leibovitz´s L15) per hour at room temperature. The extracellular recording technique of excised AMe and data analysis were described previously (Schneider and Stengl 2005a). Glass electrodes (0.3-1.5 MΩ) connected to an extracellular amplifier (NPI, Tamm, Germany) recorded the extracellular electrical activity of the excised AMe. Multiunit action potentials (=events) were recorded as upward and/or downward deflections of the baseline. The output of the amplifier was high-pass filtered (3 Hz) to eliminate electrode offset and low-pass filtered (1.5 kHz) to avoid high frequency noise and aliasing. The signal was digitized (DIGIDATA 1322A; Axon Instruments, Burlingame, CA, USA) with a sampling rate of 5 kHz. For data-reduction only activity with amplitudes above a selected threshold was stored on hard disc.

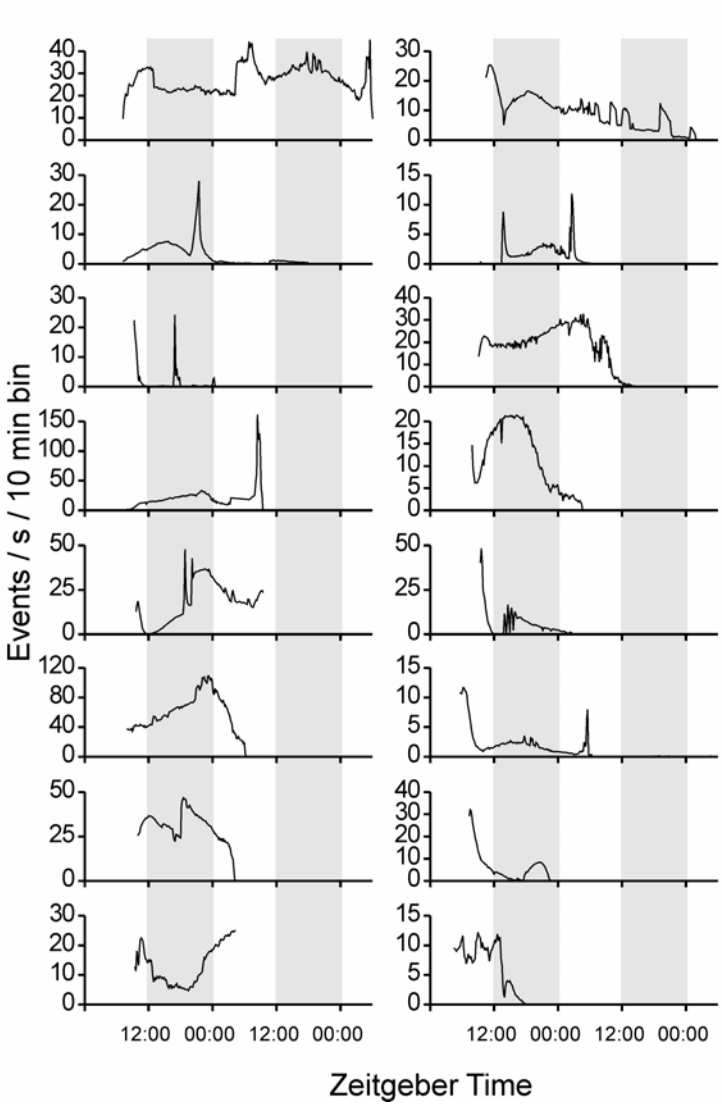

Figure 1. Maxima and minima of extracellularly recorded electrical activity of the AMe do not occur at random. Most peaks occur at the beginning, at the middle, or at the end of the light or the dark phase. The long-term recordings lasted between 12 hours and 5 days.

Therefore, the digitized signal was high-pass filtered (100 Hz) online to eliminate the offset. Spontaneous activity above the threshold triggered acquisition of a 5 ms pre- and 5 ms post-event recording (= a sweep). For offline analysis these filtered sweeps of 10 µs duration and the corresponding non-filtered sweeps were recorded. Sweeps were recorded successively in data-files of 10 min duration for rapid offline analysis. The mean frequency was calculated for every 10 min data-file. Peak values of spontaneous neural activity (activity peak) were obtained be sliding window discrimination of maximum frequency with a window width of 100 min. For activity peak distribution histograms the discriminated activity peaks then were summed in 1 hour bins of the 24 hours cycle. Sine^2 fits were performed for better visualization of periodicity (Origin 6.0; Microcal, Northhampton, CA). The circular statistics were performed using Oriana 2.02a (Kovach Computing Services, Anglesey, Great Britain). Period lengths were obtained by calculating the inter activity peak intervals. For analysis of activity peak distributions data with about the same amount of day- and night-recordings were used.

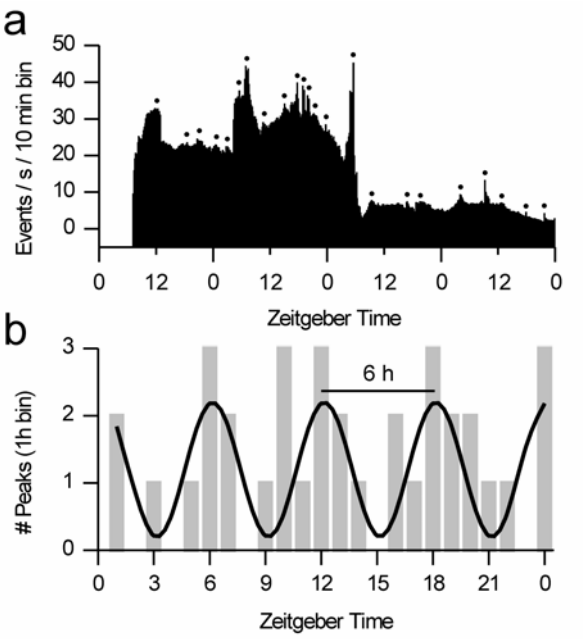

Figure 2 a-b. Distribution of activity peaks over the circadian cycle of 24 hours in a selected long-term recording. Most peaks of electrical activity occur at ZT 0, 6, 12, and 18, revealing a periodicity with τ = 6 hours. Black points indicate the appearance of activity peaks. **b** For calculation of the activity peak distribution histogram activity peak times occurring within 1 hour bins were summed and plotted against Zeitgeber time. A sine curve with a period length of 6 hours indicates the occurrence of peak accumulations every 6 hours.

Results

The extracellular multiunit recordings of animals from both inverse cultures in constant darkness (DD) were started at different Zeitgeber times and lasted between several hours up to a maximum of 5 days. Event amplitudes ranged from 50 to 150 µV, while the average peak-to-peak noise amplitude was about 40 µV. Multiunit activity comprised very variable frequency levels between 3 and 161 Hz (Fig. 1). Events were recorded as upward or downward deflections of the baseline depending on the impedance ratio between the recorded neurons, the indifferent electrode and the recording electrode. The recorded multiunit activity was reversibly blocked by superfusion of 10^{-8} M of the sodium channel blocker tetrodotoxin (n=4, not shown) within several hours after application.

For the analysis of rhythmically occurring changes of spontaneous neural activity only recordings of 12 hours minimum recording-time were evaluated with about equal amount of recordings during subjective day and night phases (n= 21). Maxima and minima of recorded multiunit activity appeared to be non-randomly distributed throughout the circadian cycle. The most predominant changes in electrical activity occurred at the beginning, the middle, or the end of the subjective light and dark phase, hinting period lengths of about 6 hours and 12 hours (Fig. 1). One recording lasted 5 days and exhibited dominant mean activity peaks with a period in the circadian range (Figs. 2). The χ^2 periodogram analysis of most predominant event frequency changes of this recording revealed a period of 21.8 h (peak-height = 6.3 % over confidence-level, peakwidth = 0.6 hours). Because the majority of the recordings did not last longer than 24 hours, or longer recordings expressed continuous run down, χ^2 square periodogram analysis was not the method of choice. Therefore, the distribution of electrical activity peaks independently of the absolute firing frequency was analyzed within a 24 hour cycle. First, the longest recording (Fig. 2a, b), then, all recordings together which covered about equal amounts of the subjective day and the subjective night were analyzed (Fig. 3a, b). The distribution of changes in electrical activity summed over the 24 hour cycle (n=5) of the 5-days recording hinted that most changes in activity occurred about every 6 hours (Fig. 2b). At night (ZT 12–0) more changes in activity appeared to occur as compared to the day (ZT 0–12) (Fig. 2b). This tendency became more apparent when all recordings were analyzed together (n=21) (Fig. 3a, b). The multiunit recordings comprised a circadian rhythm in their electrical activity peak distribution with a mean maximum at ZT 18:28 ± 7.4 h (circular SD; Rayleigh Test: p= 0.04; Fig. 3b). Additionally, ultradian rhythms were observed which generated activity peaks every 6 hours (Figs. 2b and 3a). To examine the appearance of ultradian rhythmicity in more detail we calculated the interactivity-peak-intervals (ultradian periods) for all recordings. After summing all obtained period lengths in bins of 30 min, a clear peak at about 2 hours period length became obvious followed by smaller peaks every 1.9 hours (Fig. 4). Thus, the about 6 hours periodicity which was revealed by summing all activity peaks of the

24 hours cycle appears to be caused by ultradian rhythms with a period length of about 2 hours.

Discussion

In extracellular glass-electrode recordings of isolated accessory medullae (AMae), the circadian pacemaker centers of the cockroach *L. maderae*, we examined whether activity peaks in the spontaneous electrical activity of AMe neurons occur in a rhythmic manner throughout the daily cycle. The number of peaks in event frequencies expressed a significant maximum at the middle of the subjective night and a minimum at the middle of the day. In addition, ultradian rhythms in the occurrence of changes in electrical activity were found which were multiples of about 2 hours. Thus, the isolated AMe can generate rhythms in electrical activity from the circadian scale in the range of about 24 hours down to the scales of several hours and several milliseconds.

Do maxima in activity peak distributions of circadian clock neurons predict peptide release?

Previously, mainly mean spike frequency was analyzed to search for circadian changes in information coding. Suction electrode recordings of the optical tracts of the optic lobes of the cockroach *L. maderae* revealed robust circadian rhythmicity in spontaneous electrical activity with peak mean activity during the subjective day (Colwell and Page 1990). It remained unknown whether the recorded cells resembled cells negatively or positively controlled by the circadian clock. In contrast to the cockroach, the circadian rhythm of extracellularly recorded multiunit activity of the optic lobe of the cricket *Gryllus bimaculatus* comprised maximal mean frequency during the subjective night (Tomioka and Chiba 1992). The authors focused their interest on the mean frequency of multiunit activity and predominantly evaluated rhythmicity comprising circadian periods. Since we found that changes in recorded multiunit activity of the excised AMe are apparently caused by the synchronization /desynchronization of pacemaker cell assemblies (Schneider and Stengl 2005a), we predominantly investigated the timing of activity peaks independent of the absolute mean frequency over the 24 hour cycle. As shown previously (Schneider and Stengl 2005a), the extracellularly recorded electrical events of the isolated AMe usually originate from more than one cell. They are multiunit recordings from regularly firing cells which form phase-locked assemblies that are synchronized via GABA-ergic interneurons to zero phase difference. Thus, within an assembly all synchronized cells fire action potentials at the same time. The phase-locked regularly occurring action potentials add up to higher extracellularly recorded event amplitudes which easily can be distinguished from noise (Schneider and Stengl 2005a). Changes in action potential frequencies which coincide with

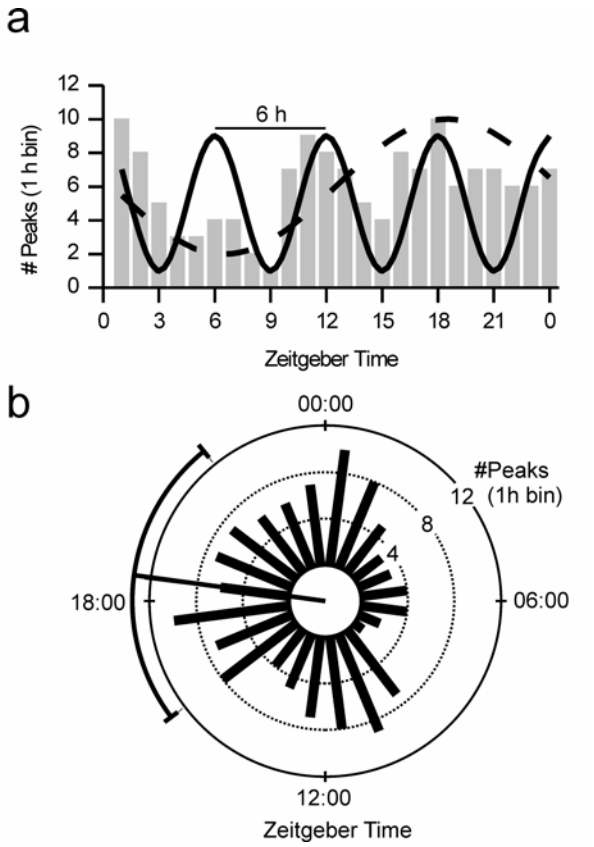

Figure 3 a-b. The spiking activity of AMe neurons exhibits a circadian rhythm. The maximum in the activity peak distribution occurs in the middle of the night and the minimum at the middle of the day. **a** Activity peak distribution histogram calculated from recordings of 20 AMae. Peaks are predominantly distributed between ZT 10 and ZT 20. The fewest peaks occur during the middle of the day. The dashed sine curve with a period length of 24 hours shows a maximum at ZT 18 and a minimum at ZT 6. Additionally an ultradian rhythm with a period length of 6 hours seems to be present (indicated by the black sine curve). **b** Circular plot of activity peak distribution. The mean activity peak time is ZT 18:28 ± 7.4 hours (circular SD; Rayleigh Test: p= 0.04), indicating a predominant activity peak distribution during the middle of the night and a minimal during the day.

changes in event amplitudes usually indicated changes in the synchronization of AMe neurons. PDF injection data suggested that peptide release gates outputs via synchronization of cells from different assemblies, causing disinhibitions of respective outputs of the clock (Schneider and Stengl 2005a). Thus, changes in synchronization of AMe neurons are accompanied with changes in event frequency and we hypothesized that peaks in event frequencies might be indicative of peptide-dependent gating. Therefore, we searched for rhythms in activity peak distribution over the 24 hours cycle to possibly predict rhythmic peptide release at particular daytimes.

Our data support the hypothesis that a large frequency of activity changes is correlated with peptide release since injections of PDF, allatotropin, GABA, and 5HT caused phase response curves with maxima around the late day, the middle and end of the night (Petri and Stengl 1997; Petri et al. 2002), in good correlation with the activity peak distribution found here. But so far, we found no peptides which caused phase shifts during the early day where the

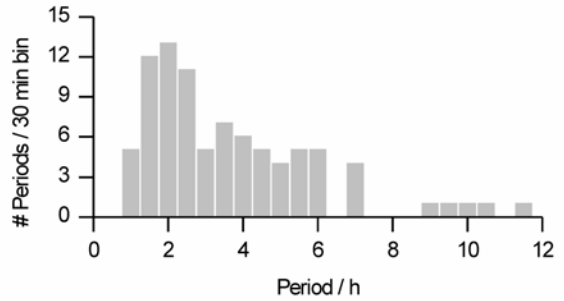

Figure 4. AMe neurons exhibit ultradian activity periods in the hour range. **a** Period lengths were gained by calculating the inter-activity peak interval and counted in 30 min bins. The histogram reveals a main period length of about 2 hours.

activity peak distribution also determined a maximum of activity changes. An analysis of rhythmic changes in spike coding in the rat SCN revealed a significant rhythm in entropy of the log interval histogram (as a measure of coding capacity) also with the most prominent peak in the mid-dark period (Bhumbra et al. 2005). Therefore, both in the insect and the mammalian circadian pacemaker center major changes in information processing take place at the middle of the night, when the overall mean electrical activity is low as compared to its maximum during the day (Inouye and Kawamura 1982; Colwell and Page 1990).

Interestingly, brain levels of the inhibitory neurotransmitter GABA in *L. maderae* vary with a circadian rhythm in constant darkness, with highest levels during the middle of the subjective day and lowest during the middle of the night (McCay et al. 1996). But it is unknown so far whether also in the AMe there is a circadian rhythm of GABA concentration. Strong GABA-ir in the AMe originates from local interneurons as well as from the input of the GABA-ir distal tract (Petri et al. 2002). The distal tract relays light entrainment information to the circadian clock in *L. maderae* which would imply more inhibitory input into the AMe during the day as compared to the night (Reischig and Stengl 1996; Lösel and Homberg 2001). Future experiments will examine whether GABA-release during the day is responsible for the minimum in activity changes during the day and whether during the middle of the night most peptides are released to gate clock outputs to different effectors.

Extracellular recorded multiunit activity comprises ultradian periods that are multiples of a fundamental 2 hours period.

In addition to the observed circadian period of rhythmic changes in multiunit activity we found ultradian rhythms with periods that are integer multiples of about 2 hours. Also Tomioka and Chiba (1992) observed activity peaks during the mid-subjective day in addition to the predominant activity peak during subjective night in *G. bimaculatus*, indicating additional oscillations with a period of 12 hours. Even for the mammalian SCN it is reported that additionally to the *in vitro* observed circadian rhythm with peak electrical activity during the mid-subjective day *in vivo* many high-frequency components are observed (Dind et al. 1994; Meijer et al. 1997; Yamazaki et al. 1998; Meyer-Spasche et al. 2002). Probably, the loss of complexity of the *in vivo* rhythm under culture conditions is due to the strong reduction of neuronal connections in cultured hypothalamic slices (Schaap et al. 2003; Bhumbra et al. 2005). Our preparation of the isolated circadian pacemaker enables us to observe circadian and ultradian periods in the action potential rhythms generated by AMe neurons despite the disruption of input and output pathways. In addition, high frequency ultradian rhythms in the gamma band range of 30-80 Hz were observed (Schneider and Stengl 2005a, b). But the source and mechanisms for the generation of the ultradian rhythms within the AMe are still obscure. In mammals ultradian rhythms of release rates of catecholamines, histamine, dopamine, adrenaline, and noradrenaline were observed (Dietl et al. 1992; Prast et al. 1992; Grass et al. 1996). Thus, possibly the circadian pacemaker center is both an ultradian and circadian clock and generates also ultradian release of neuropeptides and neurotransmitters at different phases of the circadian cycle to gate different outputs every two hours to maintain the temporal structure of physiological processes within the body. Future experiments will test whether the PERIOD-based molecular feedback loop is also responsible for the temporal precision of neuronal activtiy in the ultradian range and whether coupled ultradian rhythms generate circadian rhythms in AMe neurons in the cockroach, as suggested previously (Klevecz et al. 1991).

Acknowledgements:
We thank Dr. Jan Dolzer (Axon Instruments, Burlingame) for his help with establishing the recording technique and Dr. Thomas Reischig (University of Marburg and Göttingen) who introduced us to the isolation of accessory medullae. Additionally, we thank Dr. Thomas Schanze and Keram Pfeiffer (University of Marburg) for helpful discussions of analysis methods.

References

Bloch G, Solomon SM, Robinson GE, and Fahrbach SE. Patterns of PERIOD and pigment-dispersing hormone immunoreactivity in the brain of the European honeybee *Apis mellifera*: age- and time-related plasticity. *J Comp Neurol* 464:269-284, 2003.

Bhumbra GS, Inyushkin N, Saeb-Parsy K, Hon A, and Dyball RE. Rhythmic changes in spike coding in the rat suprachiasmatic nucleus. *J Physiol* 563: 291-307, 2005.

Colwell CS and Page TL. A circadian rhythm in neural activity can be recorded from the central nervous system of the cockroach. *J Comp Physiol A* 166: 643-649, 1990

Ding JM, Chen D, Weber ET, Faiman LE, Rea MA, and Gillette MU. Resetting the biological clock: mediation of nocturnal circadian shifts by glutamate and NO. *Science* 266: 1713-1717, 1994.

Dietl H, Prast H, and Philippu A. Pulsatile release of catecholamines in the hopothalamus of conscious rats. *Naunyn Schmiedbergs Arch Pharmacol* 347: 28-33, 1992.

Grass K, Prast H, and Philippu A. Influence of mediobasal hypothalamic lesion and catecholamine receptor antagonists on ultradian rhythm of EEG in the posterior hypothalamus of the rat. *Neurosci Lett* 207: 93-96, 1996.

Helfrich-Förster C and Homberg U. Pigment-dispersing hormone-immunoreactive neurons in the nervous system of wild-type *Drosophila melanogaster* and of several mutants with altered circadian rhythmicity. *J Comp Neurol* 337:177-190, 1993.

Helfrich-Förster C. The period clock gene is expressed in central nervous system neurons which also produce a neuropeptide that reveals the projections of circadian pacemaker cells within the brain of *Drosophila melanogaster*. *Proc Natl Acad Sci USA* 92: 612-616, 1995.

Homberg U, Würden S, Dircksen H, and Rao KR. Comparative anatomy of pigment-dispersing hormone-immunoreactive neurons in the brain of orthopteroid insects. *Cell Tissue Res* 266: 343-357, 1991.

Homberg U, Reischig T, and Stengl M. Neural organization of the circadian system of the cockroach *Leucophaea maderae*. *Chronobiol Int* 20:577-591, 2003.

Inouye ST and Kawamura H. Characteristics of a circadian pacemaker in the suprachiasmatic nucleus. *J Comp Physiol* 146: 153-160, 1982.

Klevecz RR, Pilliod J, and Bolen J. Autogenous formation of spiral waves by coupled chaotic attractors. *Chronobiol Int* 8:6-13, 1991.

Loesel R and Homberg U. Anatomy and physiology of neurons with processes in the accessory medulla of the cockroach *Leucophaea maderae*. *J Comp Neurol* 439: 193-207, 2001.

McCay J, Romero K, Gibson J, Newton J, Wilson L, Wright J, Dahl DB, and Ferrell BR. Circadian rhythm in brain gamma aminobutyric acid levels in the cockroach, *Leucophaea maderae*. *J Exp Zool* 276: 262-269, 1996.

Meijer JH, Schaap J, Watanabe K, and Albus H. Multiunit activity recordings in the suprachiasmatic nuclei: in vivo versus in vitro models. *Brain Res* 753: 322-327, 1997.

Meyer-Spasche A, Reed HE, and Piggins HD. Neurotensin phase-shifts the firing rate rhythm of neurons in the rat suprachiasmatic nuclei in vitro. *Eur J Neurosci* 16: 239-334, 2002.

Prast H, Dietl H, and Philippu A. Pulsetile release of histamine in the hypothalamus of conscious rats. *J Auton Nerv Syst* 39: 105-110, 1992.

Petri B, Stengl M, Würden S, and Homberg U. Immunocytochemical characterization of the accessory medulla in the cockroach *Leucophaea maderae*. *Cell Tissue Res* 282: 3-19, 1995.

Petri B and Stengl M. Pigment-dispersing hormone shifts the phase of the circadian pacemaker of the cockroach *Leucophaea maderae. J Neurosci* 17: 4087-4093, 1997.

Petri B and Stengl M. Presumptive insect circadian pacemakers in vitro: immunocytochemical characterization of cultured pigment-dispersing hormone-immunoreactive neurons of *Leucophaea maderae. Cell Tissue Res* 296: 635-643, 1999.

Petri B and Stengl M. Phase response curves of a model oscillator: implications for mutal coupling of paired oscillators. *J Biol Rhythms* 16: 125-141, 2001.

Petri B, Homberg U, Loesel R, and Stengl M. Evidence for a role of GABA and Mas-allatotropin in photic entrainment of the circadian clock of the cockroach *Leucophaea maderae. J Exp Biol* 205: 1459-1469, 2002.

Reischig T and Stengl M. Pigment-dispersing hormone (PDH)-immunoreactive neurons form a direct coupling pathway between the bilaterally symmetric circadian pacemakers of the cockroach *Leucophaea maderae*. *Cell Tissue Res* , 318:553-564, 2004.

Reischig T and Stengl M. Morphology and pigment-dispersing hormone immunocytochemistry of the accessory medulla, the presumptive circadian pacemaker of the cockroach *Leucophaea maderae*: a light and electronmicroscopic study. *Cell Tissue Res* 285: 306-319, 1996.

Reischig T and Stengl M. Ultrastructure of pigment-dispersing hormone-immunoreactive neurons in a three-dimensional model of the accessory medulla of the cockroach *Leucophaea maderae*. *Cell Tissue Res* 314:421-435, 2003b.

Schaap J, Pennartz CMl, and Meijer JH. Electrophysiology of the circadian pacemaker in mammals. *Chronobiol Int* 20:171-188, 2003.

Sato S, Chuman Y, Matsushima A, Tominaga Y, Shimohigashi Y, and Shimohigashi M. A circadian neuropeptide, pigment-dispersing factor-PDF, in the last-summer cicada *Meimuna opalifera*: cDNA cloning and immunocytochemistry. *Zool Sci* 19**:**821-828, 2002.

Schneider NL and Stengl, M. Pigment-dispersing factor and GABA synchronize cells of the isolated circadian clock of the cockroach *Leucophaea maderae*. *J Neurosci* 25:5138-5147, 2005a.

Schneider NL and Stengl, M. Gap junctions between accessory medulla neurons appear to synchronize circadian clock cells of the cockroach *Leucophaea*

maderae. *J Neurophysiol in press*, 2005b.

Sehadová H, Sauman I, and Sehnal F. Immunocytochemical distribution of pigment-dispersing hormone in the cephalic ganglia of polyneopteran insects. *Cell Tissue Res* 312:113-125, 2003.

Stengl M and Homberg U. Pigment-dispersing hormone-immunoreactive neurons in the cockroach *Leucophaea maderae* share properties with circadian pacemaker neurons. *J Comp Physiol* A 175:203-213, 1994.

Tomioka K. and Chiba Y. Characterization of an optic lobe pacemaker by in situ and in vitro recording of neural activity in the cricket, *Gryllus bimaculatus*. *J Comp Physiol A* 171:1-7, 1992

Yamazaki S, Kerbeshian MC, Hocker CG, Block GD, and Menaker M. Rhythmic properties of the hamster suprachiasmatic nucleus in vivo. *J Neurosci* 18: 10709-10723, 1998.

Závodská R, Sauman I, and Sehnal F. Distribution of PER protein, pigment-dispersing hormone, prothoracicotropic hormone, and eclosion hormone in the cephalic nervous system of insects. *J Biol Rhythms* 18:106-122, 2003.

Danksagung

Ich danke Frau Apl. Prof. Dr. Monika Stengl für die Betreuung meiner Doktorarbeit. Sie hat mir ermöglicht, sehr selbstständig zu arbeiten und besonders zu Beginn meiner Arbeit alle Mittel zu Verfügung gestellt, um den elektrophysiologischen Messstand aufzubauen, mit dem alle Experimente durchgeführt wurden. Insbesondere gilt ihr mein Dank für unsere zahlreichen und offenen Diskussionen, die nicht ausschließlich meine Arbeit betrafen.

Ebenso danke ich dem Zweitgutachter, Herrn Prof. Dr. Uwe Homberg, und den anderen Mitgliedern der Prüfungskommission, Frau Prof. Dr. Monika Hassel und Herrn Prof. Dr. Roland Brandl, für ihren Beitrag zum erfolgreichen Abschluss meiner Promotion.

Mein spezieller Dank gilt Dr. Jan Dolzer, dessen umfangreiche Unterstützung zum Aufbau meines Messstandes und zu meinem Verständnis der Elektrophysiologie maßgeblich beigetragen hat. Vielen Dank für die „gebetsmühlenartigen" Wiederholungen von Antworten auf immer gleiche Fragen!

Bedanken möchte ich mich auch bei Dr. Thomas Reischig, der mich in die Präparation des Schabengehirns und in die Isolierung der akzessorischen Medulla eingeführt hat.

Bei dem $\chi 2$ Experten Keram Pfeiffer bedanke ich mich für die vielen anregenden Diskussionen statistischer und elektrophysiologischer Probleme, die nicht ausschließlich in den Labors stattfanden. In diesem Zusammenhang bedanke ich mich auch bei Christian Flecke, Nico Werner Funk und Wolf Dietmar Hütteroth, deren Unterstützung auch bei „wissenschaftlichen Disputen" mit anderen Arbeitsgruppen nicht unerheblich war.

Für das sehr angenehme Klima in unserem gemeinsamen Büro mochte ich Martina Mappes und Keram Pfeiffer danken.

Der Aufbau des Messstandes wäre ohne die technische Unterstützung von Herrn Horst Schmidt nicht möglich gewesen, daher gilt auch ihm mein herzlicher Dank für die vielen und schnellen Lösungen mechanischer Probleme.

Nicht zu vergessen Manfred Lupp, der neben der Beschaffung technischer Materialien auch für die eine oder andere Radtour zu begeistern war.

Dr. Joachim Schachtner gilt mein Dank für viele nicht nur wissenschaftliche Gespräche.

Bei meiner Familie möchte ich mich für die liebevolle Unterstützung während meines gesamten Studiums bedanken. Trotz aller Umwege standen sie immer hinter mir.

Nicht zuletzt möchte ich mich bei meiner lieben Freundin Angela herzlichst bedanken. Ihre ständige Motivation und ihr Zuspruch halfen mir über viele Tiefpunkte meiner Arbeit hinweg.

Erklärung

ich versichere, dass ich meine Dissertation

Elektrophysiologische Charakterisierung des isolierten circadianen Schrittmachers der Schabe *Leucophaea maderae*

selbstständig, ohne unerlaubte Hilfe angefertigt und mich dabei keiner anderen als der von mir ausdrücklich bezeichneten Quellen und Hilfen bedient habe.

Die Dissertation wurde in der jetzigen oder einer ähnlichen Form noch bei keiner anderen Hochschule eingereicht und hat noch keinen sonstigen Prüfungszwecken gedient.

Marburg, den

(Nils-Lasse Schneider)